Marine Ecology Progress Series
June 2022, Volume 691 Pages 69-82
https://doi.org/10.3354/meps14060
https://archimer.ifremer.fr/doc/00777/88906/

Failure of bivalve foundation species recruitment related to trophic changes during an extreme heatwave event

Correia-Martins A [1], Tremblay R [1], Bec Beatrice [2], Roques C [2], Atteia Ariane [8], Gobet Angélique [3], Richard Marion [3], Hamaguchi M [4], Miyajima T [5], Hori M [4], Miron G [6], Pouvreau Stephane [7], Lagarde Franck [3, *]

[1] Institut des sciences de la mer, Université du Québec à Rimouski, 310 allée des Ursulines, Rimouski, QC G5L 3A1, Canada
[2] MARBEC, Université de Montpellier, CNRS, Ifremer, IRD, 34095 Montpellier, France
[3] MARBEC, Université de Montpellier, CNRS, Ifremer, IRD, 34200 Sète, France
[4] National Research Institute of Fisheries and Environment of Inland Sea, Fisheries Research Agency, Maruishi 2-17-5, Hatsukaichi, Hiroshima 739-0452, Japan
[5] Department of Chemical Oceanography, Atmosphere and Ocean Research Institute, University of Tokyo, Kashiwanoha 5-1-5, Kashiwa, Chiba 277-8564, Japan
[6] Département de biologie, Université de Moncton, 18 avenue Antonine-Maillet, Moncton, NB E1A 3E9, Canada
[7] LEMAR, Ifremer, CNRS, IRD, UBO, 29840 Argenton en Landunvez, France
[8] MARBEC, Université de Montpellier, CNRS, Ifremer, IRD, 34200 Sète, France

* Corresponding author : Franck Lagarde, email address : franck.lagarde@ifremer.fr

Abstract :

Bivalves are regulators of coastal lagoons and provide a wide range of ecosystem services. However, coastal lagoons are sensitive to climate change. Our objective was to describe the drivers of the cascade of ecological events that occurred during a summer heatwave and which resulted in recruitment failure of the Pacific oyster Crassostrea gigas. Results show that elevated temperatures and salinity caused a shift in planktonic food availability toward smaller taxa. These trophic changes did not affect food accumulation by oyster larvae or their fatty acid composition but did affect post-metamorphosis success, with up to 24% fewer young metamorphosed postlarvae at some sites and no development of juveniles at all sites. This resulted in the failure of oyster recruitment and in the development of tubeworms, a trophic and spatial competitor that can better ingest small particles. This knowledge suggests that, in the context of marine heatwaves, the ecological limits of oyster larvae are narrower than their physiological limits.

Keywords : Climate change, Phenology, Extreme heatwave, Bivalves, Pacific oyster, · Crassostrea gigas, Reproduction, Larval ecology, Cascade of environmental effects, Trophic changes

1. INTRODUCTION

Coastal lagoons provide a wide range of ecosystem services (Villamagna et al. 2013, Kermagoret et al. 2019, van der Schatte Olivier et al. 2020) associated with biodiversity, including bivalves that are of great ecological interest and high commercial value. Bivalves also have important regulatory functions in the ecosystem thanks to their capacity to extract particles, to regenerate and store nutrients, and to form hard biogenic structures (Smaal et al. 2018). However, because coastal lagoons are shallow and exchange with the ocean is limited, they are highly sensitive to eutrophication, heatwaves, hypoxia and acidification, as well as to the effects of global climate change (Lloret et al. 2008, Lu et al. 2018, Thomas et al. 2018). An atmospheric heatwave is defined as five consecutive days with a maximum temperature 5 °C above the 1976-2005 normal (Jouzel et al. 2014). Summer 2019 was characterized by two heatwaves of exceptional intensity in France, including the Thau Basin, one lasting from June 24 to July 7, the other from July 21 to 27. The absolute heat record for France (46 °C) was measured in Vérargues in the Herault administrative department (Météo-France 2019), which includes the Thau Basin. A 13-day period of temperature stress between June 24 and July 13 was recorded with water temperatures above 27.5 °C in the Thau lagoon (Lagarde et al. 2021, Messiaen et al. 2021). Marine heatwaves (MHW) are extreme events defined as abrupt but prolonged periods of high sea surface temperatures that can occur anywhere, at any time (Scannell et al. 2016, Schlegel et al. 2017, Hobday et al. 2018). More specifically, an abnormally warm event is considered to be a MHW if it lasts for five or more days, with temperatures higher than the 90^{th} percentile based on a 30-year historical baseline period (Hobday et al. 2016). High water temperatures increase the metabolic requirements of bivalves (Filgueira et al. 2016, Thomas & Bacher 2018). Even if temperatures remain within the species' thermal range, high temperatures

combined with variations in salinity and/or food availability, can negatively impact the life cycle of bivalves (Filgueira et al. 2016, Scanes et al. 2020, Vázquez et al. 2021).

The development of planktonic larvae of the Pacific oyster (*Crassostrea gigas*) underlies their complex life history strategy (Byrne & Przeslawski 2013, Ko et al. 2014, Dineshram et al. 2016). The context of hydroclimatic stress provides a range of environmental possibilities that need to be described in order to better understand the larvae development. Several studies suggest that global changes are disrupting plankton communities and their nutritional values by affecting the abundance, size and diversity of primary producers (Klauschies et al. 2012, Sommer et al. 2012, Trombetta et al. 2019). Generally, elevated temperatures affect phytoplankton cell size with a shift from larger to smaller species (Bec et al. 2005, Trombetta et al. 2019). Adult bivalves can assimilate small phytoplanktonic particles (Sonier et al. 2016). However, the efficiency of capture is regulated by the morphology of their gills, and efficiency is generally low when small particles such as picoplankton are present (Rosa et al. 2018). Larvae feed through a less selective velum (Bower & Meyer 1990). Marine phytoplankton species are major producers of long-chain polyunsaturated essential fatty acids (EFA) but are now predicted to decrease due to ocean warming (Hixson & Arts 2016, Colombo et al. 2017). The fatty acids docosahexaenoic acid (22:6ω3; DHA), eicosapentaenoic acid (20:5ω3; EPA) and arachidonic acid (AA) are essential for the growth and survival of marine invertebrates, particularly during their metamorphosis from pelagic larvae to benthic juveniles and ultimately, their recruitment success (Gagné et al. 2010, Bassim et al. 2015). Since EFAs are poorly biosynthesized by marine animals, their intake depends on their food (Glencross 2009, Da Costa et al. 2015). Thus, both the right size of larval food and the right fatty acid composition are essential for the recruitment success of bivalves.

The aim of this study was to identify the environmental factors and trophic conditions (Table S1 & Table S2) associated with the recruitment failure of the Pacific oyster, *Crassostrea gigas*, during a heat wave. We compared two contrasted years (2017,no heatwave and 2019, occurrence of a heatwave) at four sites in the Thau lagoon, France (Fig. 1). We hypothesize that heatwaves, characterized by high temperatures and high salinity, have a negative impact on oyster recruitment due to poor larval feeding conditions caused by changes in plankton diversity.

2. MATERIALS AND METHODS

2.1 Experimental design

Annual oyster recruitment was monitored at four experimental sites in the Thau lagoon (Southern France; Fig 1.) on the same dates, i.e. between July 24 and August 21, in 2017, and between July 2 and July 29, in 2019. The average depth of the Thau lagoon is 4 m, and the lagoon covers an area of 7 500 ha (19 km x 4.5 km) of which 20% is used for shellfish culture (oysters and mussels). The lagoon is connected to the Mediterranean Sea via a network of channels through Sète Harbor (Fiandrino et al. 2017). Two experimental sites were located inside the shellfish farming areas (Marseillan and Bouzigues) and the other two outside the shellfish farming areas (Meze and Listel) (Fig 1.).

2.2 Oyster analyses

Three sets of oyster collectors were submerged vertically 2 m below the surface at each of the four study sites in the Thau lagoon. Three different oyster settler stages (Table S1) were used to estimate benthic abundances: i) pre-settled pediveliger larvae, ii) young metamorphosed postlarvae and iii) juveniles (Arakawa 1990, Lagarde et al. 2017). The sums of abundances of pediveligers and

postlarvae are listed under "young settlers" (Table S1). The collectors were installed once the oyster's larval supply reached a density of 10 000 larvae/m^3 (Pouvreau et al. 2021). The collectors located inside the shellfish culture areas were suspended from existing farming structures. Those outside the area were suspended using a tailored mooring system (Lagarde et al. 2017, 2019). Each collector was made of 44 white PVC plastic plates (15 cm in diameter; surface area 250 cm^2) stacked on a 110 cm long tube. Two weeks after their immersion, three plates per collector were harvested [at the top (i.e., the 5^{th} from the top of the collector), in the middle (the 22^{nd}) and at the bottom (the 39^{th})] and data were pooled to assess the abundance of young settlers and fatty acid (FA) content (µg $larva^{-1}$). A similar sampling procedure was used four weeks after the collectors were immersed to assess the abundance of juveniles.

The abundance of young settlers and juveniles was assessed on the upper surface of each plate using standard 15 cm^2 sub-units. Depending on abundance, 3 to 12 sub-units were randomly selected for counting and the resulting replicates were averaged to obtain the total number of individuals per plate. Recruitment was evaluated from the abundance of juveniles and metamorphosis from the ratio of juvenile to young-settler abundances. Size at metamorphosis was estimated by measuring the prodissoconch II (PII) (Martel et al. 1995). Maximum 60 juveniles were removed from each plate sampled after the fourth week after immersion, and placed on a plasticine flange fixed on a microscope blade. Observations were made under the wide-range zoom lens of a high-resolution digital microscope Keyence (VHX 2000E, 1 µm resolution, HDR images), and the maximum dorsoventral axis was measured. This measurement corresponds to the distance between the umbo and the most distant part of the clear demarcation formed by a growth line delimiting the PII from the dissoconch shell.

The fatty acid (FA) composition of young settlers was determined using a pool of 77 to 212 individuals per replicate (2-3 replicates per site depending on pediveliger abundances). Samples were preserved in vials filled with 3 mL of dichloromethane methanol (CH_2Cl_2:MeOH, 2:1 v:v), closed with a Teflon-lined cap under nitrogen atmosphere and stored at -80 °C until analysis. Lipids were extracted by grinding in dichloromethane methanol using a modified Folch procedure (Parrish 1999). Fatty acid methyl esters (FAME) were prepared using sulfuric acid and methanol (2:98 v:v) heated at 100 °C for 10 min and using 19:0 as internal standard (Lepage & Roy 1984). Samples were purified on an activated silica gel with 1 mL of hexane ethyl acetate (v:v) to eliminate free sterols. FAME were analyzed in the full scan mode (ionic range: 50–650 m:z) on a Polaris Q ion trap coupled with a Trace GC Ultra gas chromatograph (Thermo Scientific) equipped with a TriPlus autosampler, a PTV injector and an ITQ900 mass detector (Thermo Scientific). An Omegawax 250 (Supelco) capillary column was used for separation using high purity helium. Xcalibur v.2.1 software (Thermo Scientific) was used for FAME identification and quantification with the standard reference solution (Supelco 37 Component FAME Mix and Supelco menhaden oil). Unknown peaks were identified according to their mass spectra with emphasis on FA trophic makers.

2.3 Environmental measurements

Environmental factors were measured once a week (Table S1 and Table S2) starting just after the collectors were immersed and continuing until all the plates were harvested, i.e., a total of five weeks. Temperature (°C), salinity and dissolved oxygen concentrations (mg L^{-1}) were measured at a depth of 1 m and at the bottom of the water column with an Oxi1970i WTW oximeter and an LF 197-S WTW conductivity meter.

Potential food for oysters is expressed as the concentration of total suspended particulate matter varying in size from 0.7 and 20 µm ($TPM_{0.7\text{-}20\mu m}$, mg L^{-1}). It consisted of inorganic ($PIM_{0.7\text{-}20\mu m}$, mg L^{-1}) and organic particulate matter ($POM_{0.7\text{-}20\mu m}$, mg L^{-1}). Once a week, three replicate water samples were collected at a depth of 1 m using a Ruttner Standard Water Sampler (Hydro-Bios Apparatebau) and stored at 4 °C for less than 2 hours before filtration to measure the concentrations (mg mL^{-1}) of pico and nano-seston. In 2017, 500-mL subsamples of 1-L samples were used for filtration, while on 2019, 1-L subsamples of 2-L samples were used. Water samples were first filtered by gravity through a Nuclepore membrane (20 µm pore size). Fractionated water samples were then filtered using a vacuum pressure pump (0.3 bar) on pre-weighed (Mettler Toledo XP6 microbalance) pre-combusted (at 500 °C) Whatman 25 mm GF/F filters (0.7 µm pore size). The GF/F filters were rinsed with an isotonic seawater solution of ammonium formate (38 g L^{-1} distilled water) to eliminate salt deposits and stored in Millipore™ PetriSlide™ containers at – 25 °C. The filters were dried at 70 °C for 24 h, weighed and the concentration of total particulate matter $TPM_{0.7\text{-}20\mu m}$ was determined. The filters were then combusted at 500 °C for 5 h and weighed again to determine the concentration of particulate inorganic matter ($PIM_{0.7\text{-}20\mu m}$, mg L^{-1}). The concentration of particulate organic matter ($POM_{0.7\text{-}20\mu m}$, mg L^{-1}) is the difference in weight between the dried and the combusted filter. To determine the FA content of the pico- and nano-seston (µg.mg $TPM_{0.7\text{-}20\mu m}^{-1}$), 1-L water samples collected in 2017 and 2-L water samples collected in 2019 were filtered as described above without addition of ammonium formate solution. GF/F filters were stored in 3 ml of CH_2Cl_2:MeOH (2:1 v:v) under a nitrogen atmosphere in vials closed with a Teflon-lined cap and stored at -80 °C. The mass of total fatty acids in the seston (MTFA; µg mg^{-1} POM) and its composition (% fatty

179 acids) were obtained as already described for oysters, with lipid extraction carried out by
180 sonification rather than grinding.
181
182 Plankton diversity was measured in 1 L samples collected in 2017 and in 2 L samples collected
183 weekly in 2019 with a Ruttner Standard Water Sampler (Hydro-Bios Apparatebau) at each
184 sampling site. This sampling strategy enabled 40 observations (4 sites x 5 weeks x 2 years).
185 Phytoplankton was characterized using the standard Utermöhl method NF-EN-152014, 2006 in
186 10 mL seawater samples. Abundances of 52 diatom taxa and 38 dinoflagellate taxa are expressed
187 as the number of individuals per liter. Chlorophyll *a* (Chl-*a*), *b* (Chl-*b*) and *c* (Chl-*c*) biomasses
188 were evaluated in 200 ml seawater samples filtered on Whatman GF/F membranes (0.7 µm
189 pore size) with a vacuum pressure pump (<10 cm Hg) (Bec et al. 2005, 2011). Filters were
190 stored in glass tubes at -20 °C until analysis. To determine the contribution of picophytoplankton
191 (<3 µm), nanophytoplankton (3 to 20 µm) and microphytoplankton (>20 µm), two out of three
192 samples were size-fractioned beforehand by gravity through Nuclepore membranes (3 and 20
193 µm pore size). Filters were ground in acetone (90%) and extracted at 4 °C for 24 h in the dark.
194 Pigment contents were measured with a spectrofluorometer (Perkin-Elmer LS50b) (Neveux &
195 Lantoine 1993) and are expressed in µg Chl *a* L^{-1}. Concentrations of picocyanobacteria (<1 µm),
196 autotrophic picoeukaryotes (<3 µm), nanophytoplankton (3-20 µm) and bacteria were estimated
197 using a FACSCalibur flow cytometer according to flow cytometry methods (Marie et al. 1997,
198 Bec et al. 2011). Seawater samples (1-ml) were analyzed; abundances are expressed in cells per
199 liter. Total picophytoplankton abundances were assessed by summing picocyanobacteria and
200 photosynthetic picoeukaryote abundances. Fluorescent beads (0.94 µm; 2 and 3 µm,
201 Polysciences) were added to each sample to calibrate for cell size of phytoplankton in terms of

equivalent spherical diameter. To measure bacterial abundances, seawater samples were fixed with prefiltered (0.2 μm) buffered formaldehyde (2% final concentration) and stored in liquid nitrogen. The procedure was slightly modified as higher concentrations of fluorochromes (SYBR Green I) were used (Bouvy et al. 2016). The fixed samples were incubated with SYBR Green I (Molecular Probes) at a final concentration of 1/375 at 4 °C for 15 min in the dark. Stained bacterial cells excited at 488 nm were determined according to their side-scattered light and green fluorescence collected using a 530/ 30 nm filter. Fluorescent beads (0.94 μm; Polysciences) were added to each sample as size reference beads.

Protozooplankton (heterotrophic flagellates) abundances were determined using the standard 2006 Utermöhl method NF-EN-152014, and are expressed in cells per liter. Until used for heterotrophic flagellate analysis, 30 ml seawater samples were preserved with 2.5 ml of prefiltered (0.2 μm) formaldehyde and kept at 4 °C in the dark. Before counting, 10 ml subsamples were stained with 4',6-diamidino-2-phenylindole (DAPI) to reach a final concentration of 2.5 μg ml^{-1}. Heterotrophic flagellates were counted by size class (2-5 μm, 5-10 μm and >10 μm) under an epifluorescence microscope (Olympus AX70) with UV illumination (Sherr et al. 1993).

2.4 Territorial competition

The percent cover of tubeworms (*Ficopomatus enigmaticus*) on 6 plates per site sampled in the fourth week after immersion was estimated to assess territorial competition with oyster juveniles, but only during the 2019 sampling season, as no tubeworms were observed in 2017. In 2017, each plate used for oyster sampling was checked for the presence of potential competitors, which was when the absence tubeworms was noted. Photographs of each plate

were taken with a GoPro HERO4 Silver camera equipped with a macro pro filter (San Mateo, CA, USA) and in 2019, the % of tubeworms recovered on the plate was estimated using Image-Pro Insight 9.1 software (MediaCybernetics, Rockville, MD, USA).

2.5 Statistical analyses

All PERMANOVA analyses were performed with Primer 7 and Permanova+1 (version 7.0.13) software. A two-way PERMANOVA (n perm.: 9999) was conducted using a Euclidian distance matrix to test the effect of year (2 fixed levels) and sampling site (4 fixed levels) on size at metamorphosis, total and essential fatty acid contents in young settlers, and on all the environmental variables measured, except the oxygen level, which was added as a third factor (depth) in the analysis. Homogeneity was evaluated using the permutation analysis of multivariate dispersion (PERMDISP). When significant PERMANOVAs were observed, post hoc multiple comparison tests were carried out. Multivariate analyses of total FA composition in young settlers and in seston, including *a posteriori* pairwise comparison, were done using distance-based permutational multivariate analysis of variance (PERMANOVA, 9999 permutations) based on Euclidian dissimilarities, with year (2 fixed levels) and sampling site (4 fixed levels) as sources of variation. Variations in FA composition, expressed in percentages, were visualized using non-metric multidimensional scaling (n-MDS). The similarity percentage (SIMPER) procedure was performed on untransformed data to identify the FAs that explained the most dissimilarity between significantly different levels.

3. RESULTS

3.1 Oyster recruitment

Recruitment numbers showed dramatic annual variability with great success at some sites in 2017 but an overall near-zero recruitment level at all sites in 2019 (Fig. 2a, b). In 2017, the metamorphosis survival rate, expressed as the ratio of juvenile to young settler abundances per plate, also showed marked spatial variability (Fig. 2a). The ratio of juvenile (123 ± 9 ind. plate^{-1}) to young-settler abundances per plate (49 ± 6 ind. plate^{-1}) was 2.5 in Bouzigues. However, at the other sites, the level of recruitment was 24% lower (94 ± 16 juveniles plate^{-1}) in Meze, 90% (13 ± 2 juveniles plate^{-1}) in Listel, and 97% (4 ± 2 juveniles plate^{-1}) in Marseillan. A smaller supply of larvae (6 ± 2 young-settlers plate^{-1}) was observed in Marseillan, but the metamorphosis survival rate was 0.6. However, in Meze and Listel, the low recruitment rates were not linked to the supply of larvae, as young settler abundances were higher in Meze (328 ± 71 young settler plate^{-1}, with a metamorphosis survival rate of 0.3) and in Listel (670 ± 65 young settler plate^{-1}, with a metamorphosis survival rate of 0.02) than in Bouzigues. Failure characterized the 2019 oyster recruitment season: low abundances of young settlers were observed in Meze (116 ± 5 ind. plate^{-1}) and in Listel (31 ± 2 ind. plate^{-1}), with almost 3 and 22 times fewer individuals than in 2017, respectively. This trend was not observed in Bouzigues (84 ± 9 ind. plate^{-1}) or in Marseillan (45 ± 3 ind. plate^{-1}) in 2019. Instead, young settlers were respectively 2 and 7 times higher in 2019 than in 2017. However, two weeks later, almost no juveniles were observed on the plates (average 0.14 ± 0.06 ind. plate^{-1}), regardless of the sites, pointing to a general oyster recruitment failure in 2019.

The size of the juveniles at metamorphosis (PII length) was established in all samples except in samples from Bouzigues in 2019 (Fig 2c, d), in which no metamorphosis of young settlers to juveniles was observed. PII individuals sampled in 2019 were 5.1% smaller (mean 262 ± 1 µm)

than those sampled in 2017 (mean 276 ± 1 µm). Differences among sites were only observed in 2017, when PII sizes in Bouzigues were 2.7% smaller than those in Meze ($p = 0.02$), Listel ($p = 0.01$) and Marseillan ($p = 0.03$).

No significant differences in total fatty acid (TFA) contents were observed in young settlers at the four sites and in the two years ($p > 0.05$). The overall TFA average was 51 ± 19 ng larvae^{-1}. The sum of essential fatty acids (EFA) corresponded to about 10% of TFA with an effect of year × site (pseudo-$F_{3,19}$=6.47, p=0.007), as individuals in Listel (p=0.02) and Marseillan (p=0.006) had 5 times lower EFA contents in 2017 than in 2019. The fatty acid composition of young settlers varied with the year × site interaction (pseudo-$F_{3,19}$=2.34, p=0.017), as individuals sampled in Listel (p=0.047) and Marseillan (p=0.044) had different profiles between the two years (Fig. S1). According to a SIMPER analysis, the interannual differences observed at these two sites were linked to DHA (22:6n3), EPA (20:5n3), AA (20:4n6), 18:2n6, 18:0 and 16:0 explained more than 83% of the average dissimilarity in the fatty acid profiles. DHA, EPA and AA levels in young settlers sampled in 2019 were twice higher than in 2017, while the levels of 18:2n6 were five times lower in 2019 than in 2017, except at the Meze and Bouzigues sites ($p > 0.09$).

3.2 Physicochemical parameters

Average water temperatures were 2.6 °C higher in 2019 than in 2017, respectively, 26.8 °C (the maximum temperature measured at the surface in Marseillan, (August 7, 2019, with 29.7 °C) and 24.2 °C. In the same way, salinity was 0.3 higher, respectively, 39.3 and 39.0 in 2019 than in 2017 (Fig 3a, b, Table S3 and Table S4). A site effect was also observed for salinity in the Thau lagoon. On average over the 2 years, observed salinity increased from east to west: mean

293 salinity (39.5) in Marseillan was 0.68 higher than in Bouzigues where mean salinity was 38.8.
294 Conversely, no significant difference in temperature was observed among sites although the
295 averages varied from 23.8 °C in Bouzigues to 24.5 °C in Marseillan in 2017 and from 26.3 °C
296 to 27.2 °C, respectively, in 2019. There was a site × year interaction effect on the oxygen
297 concentration (Table S5). No significant difference was observed among sites in 2017 with
298 oxygen concentrations ranging between 6.23 mg O_2 l^{-1} and 6.53 mg O_2 l^{-1} (c). The lowest mean
299 oxygen concentration, 5.64 mg O_2 l^{-1} at the surface of the lagoon and 3.52 mg O_2 l^{-1} at the
300 bottom, were observed in Bouzigues in 2019 during the heatwave ($p = 0.001$). Oxygen
301 concentrations varied with water depth, lower values were generally observed near the bottom
302 (Fig. 3c). Minimum concentrations of oxygen, i.e. below 2mg l^{-1}, were recorded as early as July
303 8, 2019 at the bottom of the lagoon in Bouzigues.
304
305 **3.3 Potential food for oyster larvae**
306 Concentrations of $TPM_{0.7\text{-}20}$, $PIM_{0.7\text{-}20}$and $POM_{0.7\text{-}20}$ were more than twice higher in 2019 than
307 in 2017 (Fig. a, b, c, Table S6, S7 and S8). Significant differences among the four sites were
308 only observed in the concentrations of $POM_{0.7\text{-}20}$. For both years, $POM_{0.7\text{-}20}$ concentrations in
309 Marseillan were 0.7 and 0.8 times lower than in Listel and Meze ($p = 0.01$ and 0.03,
310 respectively). An effect of the year × Chl-*a* biomass fraction was observed (Table S9). Mean
311 nanophytoplankton and picophytoplankton biomasses ($p = 0.0001$ and $p = 0.0004$ respectively)
312 were 3 times higher in 2019 than in 2017 (Fig.4d, e). A site × year effect was also observed,
313 Chl-*a* biomass values were 45% lower in Bouzigues than in Listel ($p=0.01$) and Meze
314 ($p = 0.004$) in 2017. In 2019, biomass in Marseillan was 62% lower than at the other sites ($p <$
315 0.02). Interannual variability in Chl-*a* biomass in Bouzigues was found to be 3 times in 2019

316 (p = 0.0007) than in 2017. Similar patterns were observed for Chl-*b* and Chl -*c* biomass, with
317 twice as much Chl-*b* in the samples collected in 2019 than in the samples collected in 2017
318 (0.069 µg L^{-1} versus 0.026 µg L^{-1}; p=0.0001), and a more than two-fold increase in Chl-*c* (0.103
319 ug L^{-1} versus 0.046 ug L^{-1}), particularly in Listel (p=0.039) and Bouzigues (p=0.0003).
320 Oysters feed primarily on nanophytoplankton and microphytoplankton based on diatoms and
321 dinoflagellates, both of which decreased in 2019 relative to 2017 in favor of picoplankton. Flow
322 cytometry data showed an effect of the year on cells smaller than 3 µm (Fig.). Abundances of
323 picoeukaryotes (< 3 µm) (Table S10), picocyanobacteria (< 1 µm) (Table S11 and S12) and
324 bacteria (Table S14) were higher in 2019 than in 2017. However, nanophytoplankton (3-20 µm)
325 abundances decreased by 39% in 2019 (Table S13). The abundance of total heterotrophic
326 flagellates did not vary significantly among sites or between years, the mean value being 2 866
327 ± 291 cell mL^{-1}. Dinoflagellate and diatom abundances were affected by the year (pseudo-
328 $F_{1,35}$=5.64, p=0.023), total values decreased by 60% in 2019 compared to 2017. These variations
329 were linked to a 93% decrease in *Chaetoceros* abundance from 184 715 ± 66 846 to 12 483 ± 3
330 540 cells L^{-1} (SIMPER contribution: 77%, pseudo-$F_{1,35}$=8.73, p=0.0001) and the disappearance
331 of *Skeletonema* in Listel and Meze between 2017 and 2019. Diatom taxa were fewer in number
332 at all sites sampled in 2019 with a maximum of 13 identified compared to 21 taxa identified in
333 2017. A marked increase in *Pseudo-nitzschia* (19 920 ± 10 513 to 50 562 ± 13 652 cells L^{-1})
334 with a SIMPER contribution of 8% and (pseudo-$F_{1,35}$=8.73, p=0.0001), *Leptocylindrus*
335 (SIMPER contribution 7%), *Thalassionema*, and *Cylindrotheca* (1 837 ± 222 to 18 712 ± 12
336 010 cells L^{-1}) was observed in 2019 compared to 2017. This trend was particularly clear in
337 Bouzigues (Fig. 6). This result also reflects the higher diversity of dinoflagellate taxa observed
338 in 2019 (16 taxa) than in 2017 (12 taxa).

TFA contents in the $TPM_{0.7\text{-}20}$ samples were twice higher in 2019 (19.2 µg mg $TPM_{0.7\text{-}20}^{-1}$) than in 2017 (9.9 µg mg $TPM_{0.7\text{-}20}^{-1}$;pseudo-$F_{1,61}$=17.1, p=0.0002) with no differences among sites and year × site effects. The fatty acid composition of the $TPM_{0.7\text{-}20}$ samples differed between years (pseudo-$F_{3,76}$=3.08, p=0.0001) and, as determined by SIMPER analysis, explained 97% of the differences in the levels of 18:1n9, 18:0, 16:1, 18:2n6, 16:0, 14:0, 20:5n3 and 22:6n3. Twenty-six percent of the difference observed between years was related to 18:1n9, an FA that was twice as abundant in 2017 (up to 24.1% of the TFA) than in 2019. The dissimilarity in the FA profiles observed between years was also explained by higher values of 18:2n6 (representing up to 10.8% of TFA), and EPA (7%) in 2017. 18:2n6 and EPA were, respectively, 11.3% and 5% higher in 2017 than in 2019. The most abundant FAs in the $TPM_{0.7\text{-}20}$ samples in 2019 were 16:1 and DHA, which explained, respectively, 13% and 4.3% of the dissimilarity revealed by SIMPER analysis.

3.4 Territorial competition by worms

The percent cover of tubeworms (*Ficopomatus enigmaticus*) on the plates in 2019 showed a marked increase in this species. Differences were observed among the sites (pseudo-$F_{3,33}$=157, p=0.0001). Results showed a similar percent cover of tubeworms (93.6 ± 1.5%) in Listel and Bouzigues and a lower percent cover in Meze (83.2 ± 2.6%) ($p < 0.032$) and in Marseillan (23.6 ± 3.7%) ($p < 0.0001$).

4. DISCUSSION

The aim of this study was to identify the environmental and trophic drivers of the decline in the recruitment of the Pacific oyster, *Crassostrea gigas*, associated with a heatwave. Our hypothesis

that a heatwave has a negative effect on oyster recruitment by altering plankton diversity is supported by our results. The year 2017 is a reference year from a hydroclimatic point of view with known ecological functioning of larval development of oysters (Lagarde et al. 2017, 2019). The larval developments led to different metamorphosis rates in the study areas that are linked to environmental cues such as the abundance of nanophytoplankton (Lagarde et al. 2017, 2018). If there are more spat than larvae, we assume 100% successful metamorphosis by competent larvae and the arrival of competent larvae from elsewhere between the two observation periods, i.e. between the 14^{th} and 28^{th} day after the collectors were installed (Lagarde et al. 2017). While oyster recruitment was normal in 2017, an unprecedented failure was observed in summer 2019 in the Mediterranean Thau lagoon. The atmospheric conditions that prevail during a heatwave have strong direct effects on marine and lagoon environments that normally provide a variety of ecosystem services and host valuable species (Sarà et al. 2021). Temperature and salinity conditions are key ecological and physiological factors for *Crassostrea* larvae (His et al. 1989b, Baldwin & Newell 1995, Devakie & Ali 2000, Troost et al. 2009). In controlled experimental conditions, the entire larval life of *C. gigas*, including metamorphosis, showed high tolerance to temperatures ranging from 17 °C to 32 °C at a salinity level of 34, with low mortality (≤10%) and a maximum growth rate at 32 °C (Rico-Villa et al. 2009). The physiological limits of temperature tolerance were therefore not reached in our experimental conditions where the average temperature was 26.8 °C during the heatwave (with a maximum of with 29.7 °C measured at the surface of the lagoon in Marseillan on August 7, 2019), so in this case, temperature was not the origin of the failure. Salinity did not drop below 38 in 2017 and 2019 recruitment season, and intermittently reached more than 40 in 2019. *Crassostrea gigas* is an estuarine organism that tolerates a wide range of salinity (Nell & Holliday 1988), but no

information is available in the literature on the upper salinity tolerance of the larval stage in real conditions. The high salinity in 2019 may represent the physiological salinity threshold for oyster larvae. Our results showed that at the time of metamorphosis (PII), the larval shell (prodissoconch) was smaller in 2019, suggesting a reduction in larval growth or more rapid achievement of metamorphosis competence in high salinity years. An optimal salinity range for larval growth up to 27 and very marked reduction in growth has been observed at 31-39 (Nell & Holliday 1988). The smaller observed PII size could be linked to growth limitation under high salinity. Interestingly, no significant effect of salinity on larval survival between 19 and 39 has been reported, but a marked reduction in larval growth rate has been observed from 30 (Helm & Millican 1977, Nell & Holliday 1988). The upper tolerance limits of oysters to high salinity ranging from 35 to 45 should thus be further tested in laboratory conditions, including interactions between high temperatures and different nutritional inputs (His et al. 1989a).

Marine bivalve populations are known to be unstable due to causes intrinsic to the population or to extrinsic causes linked to environmental conditions (Skazina et al. 2013, Reed et al. 2021). The heatwave that occurred in 2019 resulted in large quantities of particulate matter and chlorophyll biomass, but their quality appeared to be unfavorable for oyster recruitment. The failure of oyster recruitment in 2019 could thus be linked to the change in phytoplankton communities with low abundance of forage diatoms and high abundance of picoplanktonic prokaryotes and eukaryotes, of heterotrophic flagellates, as well as of the diatoms *Pseudo-Nitzschia* and *Cylindrotheca*. However, the trophic environment was not characterized by a planktonic community poor in fatty acids, in fact it was richer than in 2017. Pediveliger larvae accumulated the same quantity of fatty acids in 2017 as in 2019, but metamorphosis failures were observed at all sites. We suggest that this failure may be linked to inappropriate trophic

conditions, due to the development of picophytoplankton. These species are poorly retained by the newly developed gills of postlarvae. Our results suggest that the overabundance of small particles (picoplanktonic prokaryotes and eukaryotes) could be critical for larval settlement and metamorphosis. Higher chlorophyll biomass was observed in the nanophytoplankton fraction during the heatwave in 2019 than in 2017 (with no heatwave), indicating changes in the phytoplankton community.

The heat wave was characterized by the increasing abundances of picocyanobacteria (Bec et al. 2005, Collos et al. 2009, Derolez et al. 2020b) and decreasing abundances of nanophytoplankton. The oligotrophication trajectory of the Thau lagoon began in the early 2000s (Collos et al. 2009, Derolez et al. 2020a). This process caused a community shift due to a reduction in nutrient loads that had prevailed since the 1970s thanks to improved wastewater treatment in the watershed aimed at halting eutrophication (EC 1991a b, 2000). The reduction in nutrient loads has been amplified by a decrease in total rainfall since the 2000s due to climate change (Derolez et al. 2020a). Our results corroborate evidence that the proportion of small taxa like picoplankton, in the phytoplankton community, is increasing in coastal, marine and freshwater ecosystems in response to global warming (Daufresne et al. 2009, Mousing et al. 2014, Pinckney et al. 2015). Small phytoplankton cells have been reported to dominate in oligotrophic environments (Irwin et al. 2006).

The 2019 heatwave had a negative impact on oyster larval recruitment by shifting the phytoplankton community towards picoplankton and opening a favorable ecological window for tubeworms that compete for food and land space. In this case, the failure of recruitment seems to be more linked to the ecological conditions at the time of metamorphosis of the larvae

than to their physiological limits, which were not reached. We hypothesize that the limitations encountered by oyster larvae are ecological in the sense of the absence of trophic settlement triggers (Toupoint et al. 2012, Androuin et al. 2022), which are known to be high concentrations of diatoms and high abundance of nanophytoplankton for metamorphosis survival in the Thau Lagoon (Lagarde et al. 2017, 2018). Tubeworms are opportunistic ecosystem engineers that play an important role in determining benthic species abundance and composition (Heiman & Micheli 2010, McQuaid & Griffiths 2014). In our case, high temperatures and high salinity coincided with the development of the tubeworm *Ficopomatus enigmaticus,* triggering a shift in benthic community composition that was destructive for oyster recruitment on collectors. The feeding abilities of *F. enigmatus* make it very efficient for small particles, with high ingestion rates in the size range 2-16 µm, including diatoms (Davies et al. 1989, Bruschetti et al. 2008), which exert strong top-down trophic control (Pan & Marcoval 2014). We consequently hypothesize that tubeworms are important territorial competitors and trophic competitors of oyster larvae in shallow water and brackish habitats that develop in the context of heatwaves.

This study demonstrates, for the first time, an ecological process leading to the recruitment failure of the Pacific oysters due to an extreme heatwave. The oligotrophication trajectory of our study site combined with the effects of high water temperatures caused a shift of phytoplankton communities towards small species of picophytoplankton including cyanobacteria, but that are likely unfavorable for the successful larval development of oysters until their juvenile metamorphosis (Lagarde et al. 2017). The present study thus reveals the ecological limits of the recruitment process of the Pacific oyster in the context of a heatwave in a Mediterranean lagoon. The heatwave phenomenon observed in 2019 severely disrupted the reproductive cycle of oysters in the Thau lagoon. In this context, the oyster nursery function in

an oyster farming ecosystem can only be achieved or maintained when pico-, nano- and microphytoplankton communities are present and abundant and oysters can find favorable areas for larval development and optimize their recruitment. This study provides evidence that, in the conditions created by a heatwave, the ecological limits of Pacific oyster larvae are narrower than their physiological limits. The effects of climate change, particularly the warming of waters in semi-enclosed basins, will certainly lead to problems in larval harvesting in the near future. The information included in this paper should help adapt oyster aquaculture, including husbandry practices, to a future marked by climate change.

5. Data and code availability

All the data used in the current study and the scripts used in our analysis are publicly available or were obtained by the corresponding author. This research benefited from the VELYGER Database: The Oyster Larvae Monitoring French Project (http://doi.org/10.17882/41888) and REPHY Dataset - French Observation and Monitoring program for Phytoplankton and Hydrology in coastal waters. Metropolitan data. SEANOE (https://doi.org/10.17882/47248).

6. REFERENCES

Androuin T, Barbier P, Forêt M, Meziane T, Thomas M, Archambault P, Winkler G, Tremblay R, Olivier F (2022) Pull the trigger: interplay between benthic and pelagic cues driving the early recruitment of a natural bivalve assemblage. Ecosphere 13:e03672.

Arakawa KY (1990) Natural Spat Collecting in the Pacific Oyster *Crassostrea gigas* (Thunberg). Mar Behav Physiol 17:95–128.

Baldwin BS, Newell RI (1995) Feeding rate responses of oyster larvae (*Crassostrea virginica*)

476 to seston quantity and composition. J Exp Mar Bio Ecol 189:77–91.
477 Bassim S, Chapman RW, Tanguy A, Moraga D, Tremblay R (2015) Predicting growth and
478 mortality of bivalve larvae using gene expression and supervised machine learning. Comp
479 Biochem Physiol - Part D Genomics Proteomics 16:59–72.
480 Bec B, Collos Y, Souchu P, Vaquer A, Lautier J, Fiandrino A, Benau L, Orsoni V, Laugier T
481 (2011) Distribution of picophytoplankton and nanophytoplankton along an anthropogenic
482 eutrophication gradient in French Mediterranean coastal lagoons. Aquat Microb Ecol
483 63:29–45.
484 Bec B, Husseini-Ratrema J, Collos Y, Souchu P, Vaquer A (2005) Phytoplankton seasonal
485 dynamics in a Mediterranean coastal lagoon: Emphasis on the picoeukaryote community.
486 J Plankton Res 27:881–894.
487 Bouvy M, Got P, Domaizon I, Pagano M, Leboulanger C, Bouvier C, Carre C, Roques C, Dupuy
488 C (2016) Plankton communities in the five Iles Eparses (Western Indian Ocean) considered
489 to be pristine ecosystems. Acta oecologica- Int J Ecol 72:9–20.
490 Bower SM, Meyer SG (1990) Atlas of anatomy and histology of larvae and early juvenile stages
491 of Japanese scallop *Patinopecten yessoensis*. Can Spec Publ Fish Aquat Sci 111:1–51.
492 Bruschetti M, Luppi T, Fanjul E, Rosenthal A, Iribarne O (2008) Grazing effect of the invasive
493 reef-forming polychaete Ficopomatus enigmaticus (Fauvel) on phytoplankton biomass in
494 a South West Atlantic coastal lagoon. J Exp Mar Bio Ecol 354:212–219.
495 Byrne M, Przeslawski R (2013) Multistressor impacts of warming and acidification of the ocean
496 on marine invertebrates' life histories. Integr Comp Biol 53:582–596.
497 Collos Y, Bec BB, Jauzein C, Abadie E, Laugier T, Lautier J, Pastoureaud A, Souchu P, Vaquer
498 A (2009) Oligotrophication and emergence of picocyanobacteria and a toxic dinoflagellate

499 in Thau lagoon, southern France. J Sea Res 61:68–75.
500 Colombo SM, Wacker A, Parrish CC, Kainz MJ, Arts MT (2017) A fundamental dichotomy in
501 long-chain polyunsaturated fatty acid abundance between and within marine and terrestrial
502 ecosystems. Environ Rev 25:163–174.
503 Da Costa F, Robert R, Quéré C, Wikfors GH, Soudant P (2015) Essential fatty acid assimilation
504 and synthesis in larvae of the bivalve *Crassostrea gigas*. Lipids 50:503–511.
505 Daufresne M, Lengfellner K, Sommer U (2009) Global warming benefits the small in aquatic
506 ecosystems. Proc Natl Acad Sci 106:12788 LP – 12793.
507 Davies BR, Stuart V, de Villiers M (1989) The filtration activity of a serpulid polychaete
508 population *Ficopomatus enigmaticus* (Fauvel) and its effects on water quality in a coastal
509 marina. Estuar Coast Shelf Sci 29:613–620.
510 Derolez V, Malet N, Fiandrino A, Lagarde F, Richard M, Ouisse V, Bec B, Aliaume C (2020a)
511 Fifty years of ecological changes: Regime shifts and drivers in a coastal Mediterranean
512 lagoon during oligotrophication. Sci Total Environ 732:139292.
513 Derolez V, Soudant S, Malet N, Chiantella C, Richard M, Abadie E, Aliaume C, Bec B (2020b)
514 Two decades of oligotrophication: evidence for a phytoplankton community shift in the
515 coastal lagoon of Thau (Mediterranean Sea, France). Estuar Coast Shelf Sci:106810.
516 Devakie MN, Ali AB (2000) Salinity-temperature and nutritional effects on the setting rate of
517 larvae of the tropical oyster, *Crassostrea iredalei* (Faustino). Aquaculture 184:105–114.
518 Dineshram R, Chandramouli K, Ko GWK, Zhang H, Qian PY, Ravasi T, Thiyagarajan V (2016)
519 Quantitative analysis of oyster larval proteome provides new insights into the effects of
520 multiple climate change stressors. Glob Chang Biol 22:2054–2068.
521 EC (1991a) Council Directive 91/271/EEC concerning urban waste-water treatment. Official

522 Journal L 135, 30.5.1991, p. 40–52.
523 EC (1991b) Council Directive 91/676/EEC of 12 December 1991 concerning the protection of
524 waters against pollution caused by nitrates from agricultural sources. Official Journal L
525 375 , 31/12/1991 P. 0001 - 0008.
526 EC (2000) Directive 200/60/EC of the european parliament and of the council of 23 october
527 2000 establishing a framework for community action in the field of water policy.
528 Fiandrino A, Ouisse V, Dumas F, Lagarde F, Pete R, Malet N, Le Noc S, de Wit R (2017)
529 Spatial patterns in coastal lagoons related to the hydrodynamics of seawater intrusion. Mar
530 Pollut Bull 119:132–144.
531 Filgueira R, Guyondet T, Comeau LA, Tremblay R (2016) Bivalve aquaculture-environment
532 interactions in the context of climate change. Glob Chang Biol 22:3901–3913.
533 Gagné R, Tremblay R, Pernet F, Miner P, Samain JF, Olivier F (2010) Lipid requirements of
534 the scallop *Pecten maximus* (L.) during larval and post-larval development in relation to
535 addition of *Rhodomonas salina* in diet. Aquaculture 309:212–221.
536 Glencross BD (2009) Exploring the nutritional demand for essential fatty acids by aquaculture
537 species. 71–124.
538 Heiman KW, Micheli F (2010) Non-native Ecosystem Engineer Alters Estuarine Communities.
539 Integr Comp Biol 50:226–236.
540 Helm MM, Millican PF (1977) Experiments in the hatchery rearing of Pacific oyster larvae.
541 Aquaculture 11:1–12.
542 His E, Robert R, Dinet A (1989a) Combined effect of temperature and salinity on fed and
543 starved larvae of the Mediterranean mussel *Mytilus galloprovincialis* and the Japanese
544 oyster *Crassostrea gigas*. Mar Biol 100:455–463.

His E, Robert R, Dinet A (1989b) Marine biology of the Mediterranean mussel *Mytilus galloprovincialis* and the Japanese oyster *Crassostrea gigas*. Mar Biol 100:455–463.

Hixson SM, Arts MT (2016) Climate warming is predicted to reduce omega-3, long-chain, polyunsaturated fatty acid production in phytoplankton. Glob Chang Biol 22:2744–2755.

Hobday AJ, Alexander L V., Perkins SE, Smale DA, Straub SC, Oliver ECJ, Benthuysen JA, Burrows MT, Donat MG, Feng M, Holbrook NJ, Moore PJ, Scannell HA, Sen Gupta A, Wernberg T (2016) A hierarchical approach to defining marine heatwaves. Prog Oceanogr 141:227–238.

Hobday AJ, Oliver ECJ, Gupta A Sen, Benthuysen JA, Burrows MT, Donat MG, Holbrook NJ, Moore PJ, Thomsen MS, Wernberg T, Smale DA (2018) Categorizing and naming marine heatwaves. Oceanography 31:162–173.

Irwin AJ, Finkel Z V., Schofield OME, Falkowski PG (2006) Scaling-up from nutrient physiology to the size-structure of phytoplankton communities. J Plankton Res 28:459–471.

Jouzel J, Ouzeau G, Déqué M, Jouini M, Planton S, Vautard R (2014) Le climat de la France au XXIe siècle (Volume 4), Scénarios régionalisés: édition 2014 pour la métropole et les régions d'outre-mer.

Kermagoret C, Claudet J, Derolez V, Nugues MM, Ouisse V, Quillien N, Baulaz Y, Le Mao P, Scemama P, Vaschalde D, Bailly D, Mongruel R (2019) How does eutrophication impact bundles of ecosystem services in multiple coastal habitats using state-and-transition models. Ocean Coast Manag 174:144–153.

Klauschies T, Bauer B, Aberle-Malzahn N, Sommer U, Gaedke U (2012) Climate change effects on phytoplankton depend on cell size and food web structure. Mar Biol 159:2455–

568 2478.
569 Ko GWK, Dineshram R, Campanati C, Chan VBS, Havenhand J, Thiyagarajan V (2014)
570 Interactive Effects of Ocean Acidification, Elevated Temperature, and Reduced Salinity
571 on Early-Life Stages of the Pacific Oyster. Environ Sci Technol 48:10079–10088.
572 Lagarde F, Atteia Van Lis A, Gobet A, Richard M, Behzad M, Roques C, Foucault E, Messiaen
573 G, Hubert C, Cimiterra N, Derolez V, Bec B (2021) Phénomène d'Eaux Vertes à
574 *Picochlorum* en lagune de Thau pendant les années 2018 et 2019. Observations
575 environnementales. FRANCE.
576 Lagarde F, Fiandrino A, Ubertini M, Roque d'Orbcastel E, Mortreux S, Chiantella C, Bec B,
577 Bonnet D, Roques C, Bernard I, Richard M, Guyondet T, Pouvreau S, Lett C (2019)
578 Duality of trophic supply and hydrodynamic connectivity drives spatial patterns of Pacific
579 oyster recruitment. Mar Ecol Prog Ser 632:81–100.
580 Lagarde F, Richard M, Bec B, Roques C, Mortreux S, Bernard I, Chiantella C, Messiaen G,
581 Nadalini J-BB, Hori M, Hamaguchi M, Pouvreau S, Roque d'Orbcastel E, Tremblay R
582 (2018) Trophic environments influence size at metamorphosis and recruitment
583 performance of the Pacific oyster. Mar Ecol Prog Ser 602:135–153.
584 Lagarde F, Roque E, Ubertini M, Mortreux S, Bernard I, Fiandrino A, Chiantella C, Bec B,
585 Roques C, Bonnet D, Miron G, Richard M, Pouvreau S, Lett C (2017) Recruitment of the
586 Pacific oyster *Crassostrea gigas* in a shellfish-exploited Mediterranean lagoon : discovery,
587 driving factors and a favorable environmental window. Mar Ecol Prog Ser 578:1–17.
588 Lepage G, Roy CC (1984) Improved recovery of fatty acid through direct transesterification
589 without prior extraction or purification. J Lipid Res 25:1391–1396.
590 Lloret J, Marín A, Marín-Guirao L (2008) Is coastal lagoon eutrophication likely to be

591 aggravated by global climate change? Estuar Coast Shelf Sci 78:403–412.
592 Lu Y, Yuan J, Lu X, Su C, Zhang Y, Wang C, Cao X, Li Q, Su J, Ittekkot V, Garbutt RA, Bush
593 S, Fletcher S, Wagey T, Kachur A, Sweijd N (2018) Major threats of pollution and climate
594 change to global coastal ecosystems and enhanced management for sustainability. Environ
595 Pollut 239:670–680.
596 Marie D, Partensky F, Jacquet S, Vaulot D (1997) Enumeration and cell cycle analysis of natural
597 populations of marine picoplankton by flow cytometry using the nucleic acid stain SYBR
598 Green I. Appl Environ Microbiol 63:186–193.
599 Martel A, Hynes TMT, Buckland-Nicks J (1995) Prodissoconch morphology, planktonic shell
600 growth, and site at metamorphosis in *Dreissena polymorpha*. Can J Zool 73:1835–1844.
601 McQuaid KA, Griffiths CL (2014) Alien reef-building polychaete drives long-term changes in
602 invertebrate biomass and diversity in a small, urban estuary. Estuar Coast Shelf Sci
603 138:101–106.
604 Messiaen G, Mortreux S, Le Gall P, Crottier A, Lagarde F (2021) Marine environmental station
605 database of Thau lagoon.
606 Météo-France (2019) 46,0 °C à Vérargues : nouveau record officiel de température observée en
607 France. http://www.meteofrance.fr/actualites/74345599-c-est-officiel-on-a-atteint-les-46-
608 c-en-france-en-juin
609 Mousing EA, Ellegaard M, Richardson K (2014) Global patterns in phytoplankton community
610 size Structure-evidence for a direct temperature effect. Mar Ecol Prog Ser 497:25–38.
611 Nell JA, Holliday JE (1988) Effects of salinity on the growth and survival of Sydney rock oyster
612 (*Saccostrea commercialis*) and Pacific oyster (*Crassostrea gigas*) larvae and spat.
613 Aquaculture 68:39–44.

Neveux J, Lantoine F (1993) Spectrofluorometric assay of chlorophylls and phaeopigments using the least squares approximation technique. Deep Res Part I 40:1747–1765.

Pan J, Marcoval MA (2014) Top-down effects of an exotic serpulid polychaete on natural plankton assemblage of estuarine and brackish systems in the south west atlantic. J Coast Res 30:1226–1235.

Parrish CC (1999) Determination of total lipid, lipid classes, and fatty acids in aquatic samples. Lipids Freshw Ecosyst:4–20.

Pinckney JL, Benitez-Nelson CR, Thunell RC, Muller-Karger F, Lorenzoni L, Troccoli L, Varela R (2015) Phytoplankton community structure and depth distribution changes in the Cariaco Basin between 1996 and 2010. Deep Sea Res Part I Oceanogr Res Pap 101:27–37.

Pouvreau S, Maurer D, Auby I, Lagarde F, Le Gall P, Cochet H, Bouquet A-L, Geay A, Mille D (2021) VELYGER Database: The Oyster Larvae Monitoring French Project.

Reed AJ, Godbold JA, Solan M, Grange LJ (2021) Reproductive traits and population dynamics of benthic invertebrates indicate episodic recruitment patterns across an Arctic polar front. Ecol Evol 11:6900–6912.

Rico-Villa B, Pouvreau S, Robert R (2009) Influence of food density and temperature on ingestion, growth and settlement of Pacific oyster larvae, *Crassostrea gigas*. Aquaculture 287:395–401.

Rosa M, Ward JE, Shumway SE (2018) Selective Capture and Ingestion of Particles by Suspension-Feeding Bivalve Molluscs: A Review. J Shellfish Res 37:727–746.

Sarà G, Giommi C, Giacoletti A, Conti E, Mulder C, Mangano MC (2021) Multiple climate-driven cascading ecosystem effects after the loss of a foundation species. Sci Total Environ 770:144749.

637 Scanes E, Parker LM, O'Connor WA, Dove MC, Ross PM (2020) Heatwaves alter survival of
638 the Sydney rock oyster, Saccostrea glomerata. Mar Pollut Bull 158:111389.
639 Scannell HA, Pershing AJ, Alexander MA, Thomas AC, Mills KE (2016) Frequency of marine
640 heatwaves in the North Atlantic and North Pacific since 1950. Geophys Res Lett 43:2069–
641 2076.
642 van der Schatte Olivier A, Jones L, Vay L Le, Christie M, Wilson J, Malham SK (2020) A
643 global review of the ecosystem services provided by bivalve aquaculture. Rev Aquac 12:3–
644 25.
645 Schlegel RW, Oliver ECJ, Wernberg T, Smit AJ (2017) Nearshore and offshore co-occurrence
646 of marine heatwaves and cold-spells. Prog Oceanogr 151:189–205.
647 Sherr EB, Caron DA, Sherr BF (1993) Staining of heterotrophic protists for visualization via
648 epifluorescence microscopy. In: *Handbook of Methods in Aquatic Microbial Ecology*, 1st
649 Editio. Kemp PF, Sherr BF, Sherr EB, Cole JJ (eds) Lewis Publishers, p 213–227
650 Skazina M, Sofronova E, Khaitov V (2013) Paving the way for the new generations: *Astarte*
651 *borealis* population dynamics in the White Sea. Hydrobiologia 706:35–49.
652 Smaal AC, Ferreira JG, Grant J, Petersen JK, Strand Ø (2018) Goods and services of marine
653 bivalves, Springer O. Cham, Switzerland.
654 Sommer U, Adrian R, Bauer B, Winder M (2012) The response of temperate aquatic ecosystems
655 to global warming: novel insights from a multidisciplinary project. Mar Biol 159:2367–
656 2377.
657 Sonier R, Filgueira R, Guyondet T, Tremblay R, Olivier F, Meziane T, Starr M, LeBlanc AR,
658 Comeau LA (2016) Picophytoplankton contribution to *Mytilus edulis* growth in an
659 intensive culture environment. Mar Biol 163:1–15.

660 Thomas Y, Bacher C (2018) Assessing the sensitivity of bivalve populations to global warming
661 using an individual-based modelling approach. Glob Chang Biol:1–18.
662 Thomas Y, Cassou C, Gernez P, Pouvreau S (2018) Oysters as sentinels of climate variability
663 and climate change in coastal ecosystems. Environ Res Lett 13:104009.
664 Toupoint N, Gilmore-Solomon L, Bourque FFF, Myrand B, Pernet F, Olivier FFF, Tremblay
665 RRR, Gilmore-Solomon L, Bourque FFF, Myrand B, Pernet F, Olivier FFF, Tremblay
666 RRR, Mohit V, Linossier I, Bourgougnon N, Myrand B, Olivier FFF, Lovejoy C, Tremblay
667 RRR, Gilmore-Solomon L, Bourque FFF, Myrand B, Pernet F, Olivier FFF, Tremblay
668 RRR (2012) Match/mismatch between the Mytilus edulis larval supply and seston quality:
669 Effect on recruitment. Ecology 93:1922–1934.
670 Trombetta T, Vidussi F, Mas S, Parin D, Simier M, Mostajir B (2019) Water temperature drives
671 phytoplankton blooms in coastal waters. PLoS One 14:1–28.
672 Troost K, Gelderman E, Kamermans P, Smaal AC, Wolff WJ (2009) Effects of an increasing
673 filter feeder stock on larval abundance in the Oosterschelde estuary (SW Netherlands). J
674 Sea Res 61:153–164.
675 Vázquez E, Woodin SA, Wethey DS, Peteiro LG, Olabarria C (2021) Reproduction Under
676 Stress: Acute Effect of Low Salinities and Heat Waves on Reproductive Cycle of Four
677 Ecologically and Commercially Important Bivalves. Front Mar Sci 8:1–19.
678 Villamagna AM, Angermeier PL, Bennett EM (2013) Capacity, pressure, demand, and flow: A
679 conceptual framework for analyzing ecosystem service provision and delivery. Ecol
680 Complex 15:114–121.
681

682 ## 7. ACKNOWLEDGEMENTS

683 The authors are grateful to the three reviewers who kindly and constructively reviewed our
684 manuscript. This research was supported by the Natural Sciences and Engineering Research
685 Council of Canada (NSERC-Discovery Grant no.299100) to R.T and by the *Ressources*
686 *Aquatiques Québec* Research Network (*Fonds de Recherche du Québec-Nature et*
687 *Technologies*, #2014-RS-171172) and MITACS (FR37656) for the internships of ACM during
688 her stay at IFREMER. This research was also funded by the VELYGER network. F.L. and R.T.
689 thank the RECHAGLO international research group, co-funded by Ifremer and the Department
690 of Fisheries and Oceans (DFO), and the *Institut France-Québec pour la coopération scientifique*
691 *en appui au secteur Maritime* (IFQM) for encouragement, support, and exchanges with Canada.
692 F.L., M.H. T.M. and M.H. thank FREA, JSPS and Campus France/Ministry of Foreign Affairs
693 for funding the scientific exchange needed for this study and the development of all the ideas
694 presented by our group.
695 We thank Hélène Cochet, Serge Mortreux, Anaïs Crottier, Grégory Messiaen, Clarisse Hubert,
696 Nabila Guenineche, Gabriel Devique, Hervé Violette, Elise Hatey, Camille Gianaroli and
697 Nathalie Gauthier for logistic support in the field and technical contributions in the laboratory.
698

699 8. AUTHOR CONTRIBUTIONS

700 A.C.M. was involved in investigation, methodology, writing, data curation, formal analysis, and
701 visualization. R.T. and F.L. were involved in conceptualization, funding acquisition,
702 investigation, methodology, writing, data curation, formal analysis, visualization, and project
703 administration. S.P. was involved in conceptualization, funding acquisition, investigation,
704 methodology, writing and project administration. B.B was involved in conceptualization,

funding acquisition, investigation, methodology, writing, data curation, formal analysis, and visualization. C.R. contributed to funding acquisition, methodology, writing, data curation and formal analysis. A.A and A.G. contributed to writing and interpretation. G.M. contributed to funding acquisition, investigation, methodology, writing and formal analysis. M.R., M.Ho, M.Ha. and T.M. contributed to conceptualization, investigation, methodology and writing.

9. COMPETING INTERESTS

The authors have no competing interests to declare.

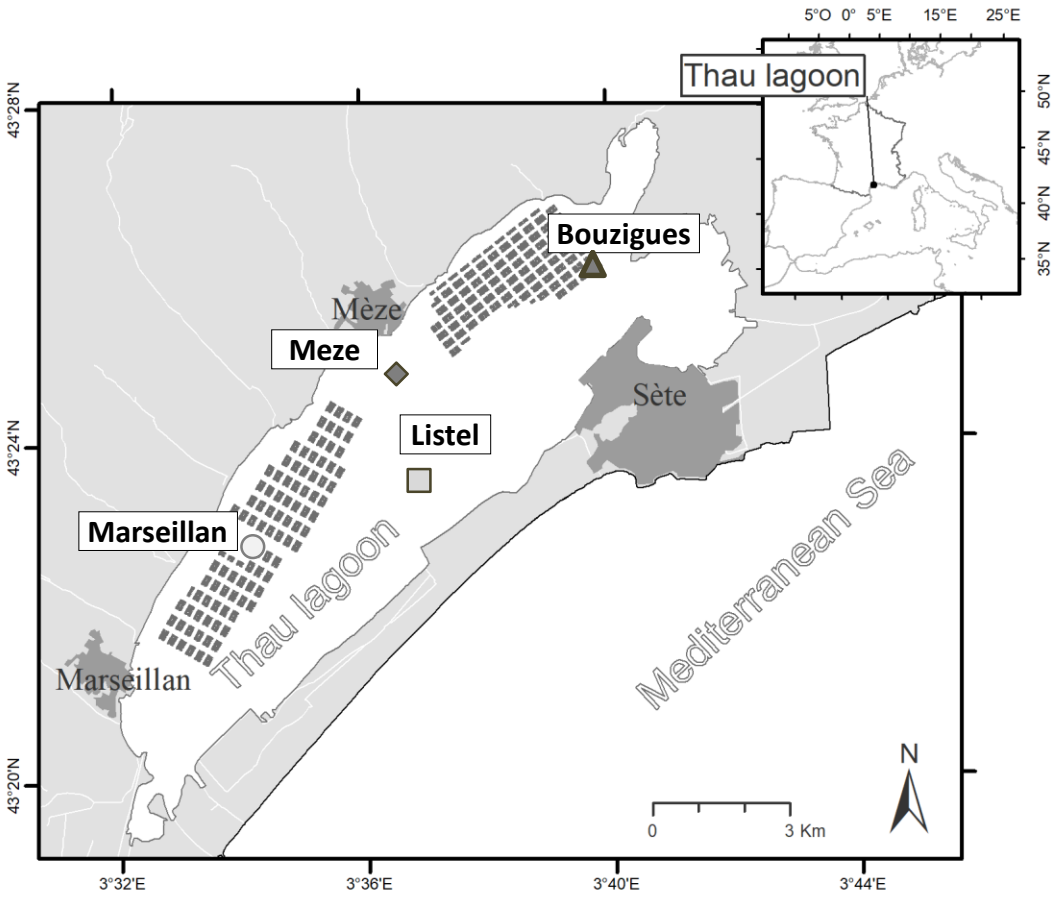

Fig. 1. The four sampling sites in the Thau lagoon. Marseillan and Bouzigues are located in the shellfish farming area; shaded areas indicate the location of shellfish culture areas. Meze and Listel are located outside the shellfish farming area.

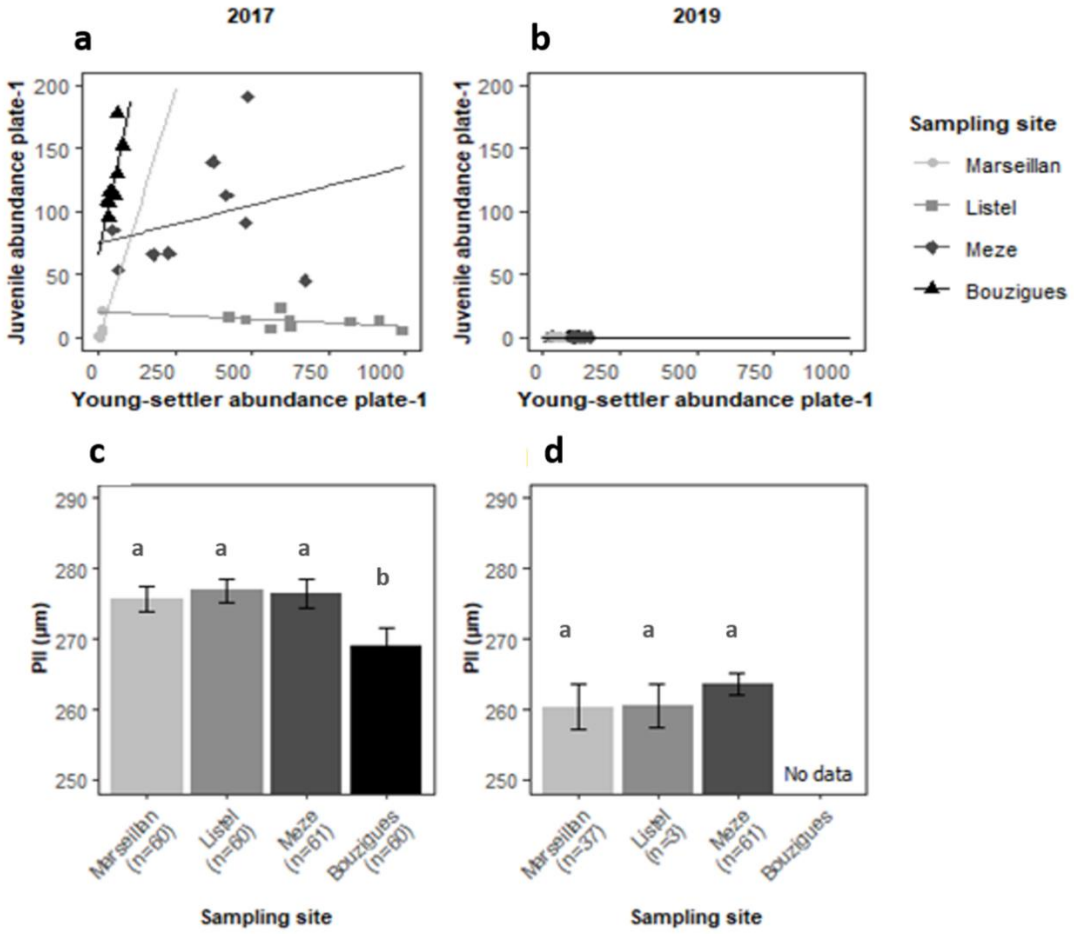

718

719 Fig. 2. Variability of oyster recruitment and prodissoconch II size in 2017 (no heatwave) and
720 2019 (heatwave). *Crassostrea gigas* recruitment performance with young settlers (pediveligers
721 + post-larvae) and juvenile abundance per collector plate observed at the four sampling sites
722 during the summer recruitment events in (a) 2017 and in (b) 2019. Size at metamorphosis was
723 estimated based on the length of prodissoconch II shell (PII, µm ± SE) of juveniles sampled in
724 (c) 2017 and (d) 2019. Different letters indicate significant differences between sites according
725 to post-hoc multiple comparison tests after PERMANOVA.

726

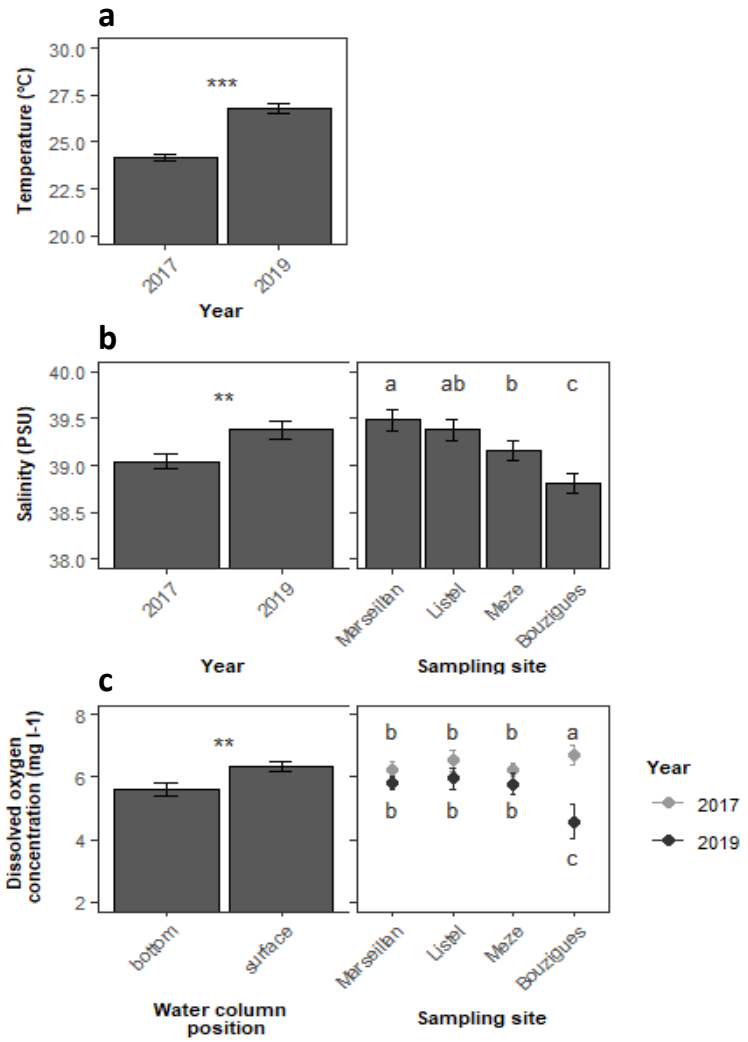

727

728 Fig. 3. Physicochemical monitoring in 2017 (no heatwave) and 2019 (heatwave). (a) Mean
729 temperature (°C ± SE) per year (n = 40), (b) mean salinity (PSU ± SE) per year (n = 40) and per
730 sampling site (n = 20) and (c) mean dissolved oxygen concentration (mg L^{-1} ± SE) according to
731 the position of the sample in the water column (n = 40) and per year and sampling site (n = 10).
732 Asterisks indicate significant differences in average parameters per year (* $p \leq 0.05$, ** $p \leq 0.01$,
733 *** $p \leq 0.001$). Different letters indicate significant differences between sites according to post
734 hoc multiple comparison tests after PERMANOVA.

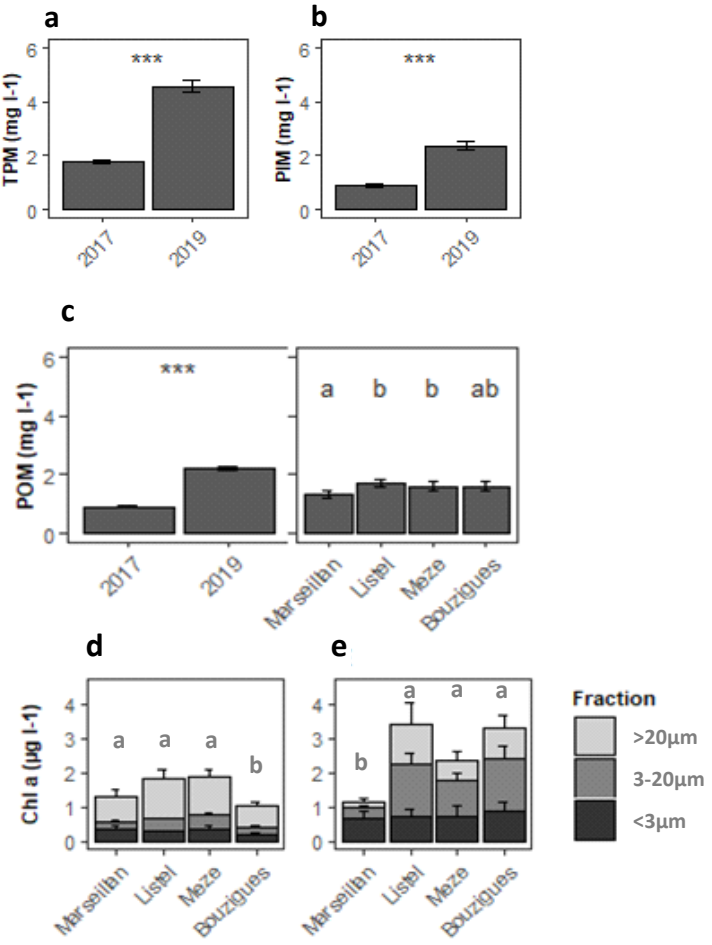

Fig. 4. Hydrobiological monitoring in 2017 (no heatwave) and 2019 (heatwave). Mean concentrations of (a) total particulate matter (TPM, mg L^{-1} ± SE), (b) particulate inorganic matter (PIM, mg L^{-1} ± SE) and (c) particulate organic matter (POM, mg L^{-1} ± SE) per year and sampling site (n = 5 per sampling site and year). Mean concentrations of chlorophyll-a (d, 2017 and e; 2019; µg L^{-1} ± SE), found in the picophytoplankton fraction (< 3 µm), the nanophytoplankton fraction (3 to 20 µm) and the microphytoplankton fraction (> 20 µm) per year and sampling site (n = 5 per sampling site, year and phytoplankton fraction). Asterisks indicate significant differences according to the average parameters per year (* $p \leq 0.05$, ** $p \leq 0.01$, *** $p \leq 0.001$). Different letters indicate significant differences between sites according to post-hoc multiple comparison tests after PERMANOVA.

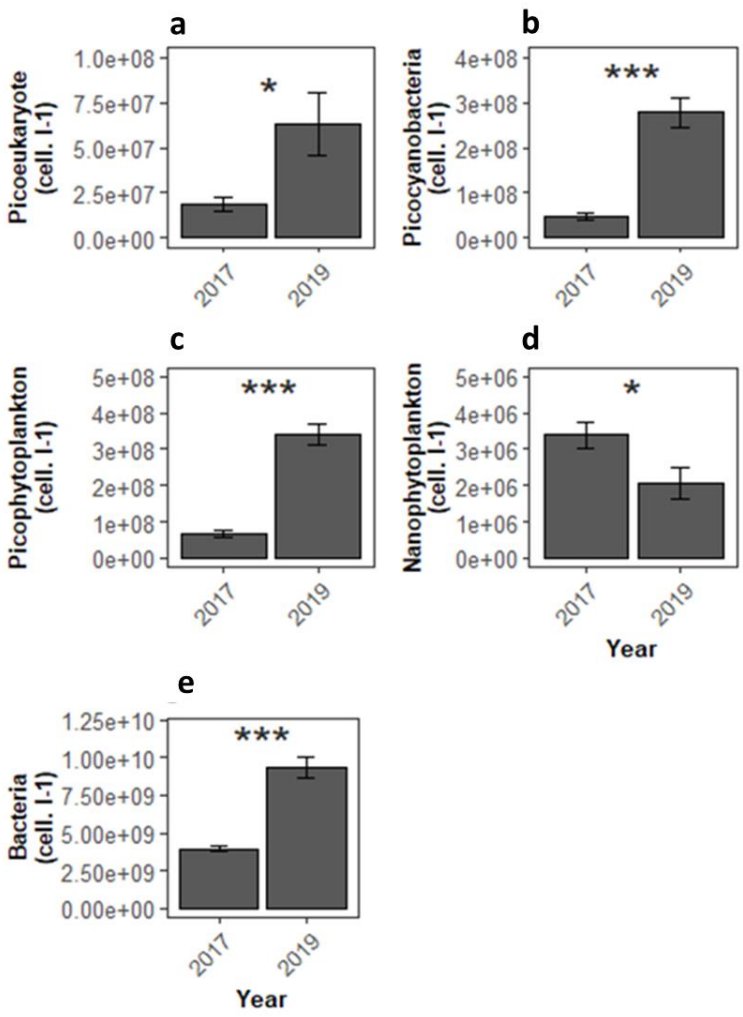

Fig. 5: Monitoring of picophytoplankton population in 2017 (no heatwave) and 2019 (heatwave). Average abundances for all sites of (a) photosynthetic picoeukaryotes, (b) picocyanobacteria, (c) picophytoplankton, (d) nanophytoplankton and (e) bacteria (cells L^{-1} ± SE) per year (n=20). Asterisks indicate significant differences according to the average parameters per year (* $p \leq 0.05$, ** $p \leq 0.01$, *** $p \leq 0.001$).

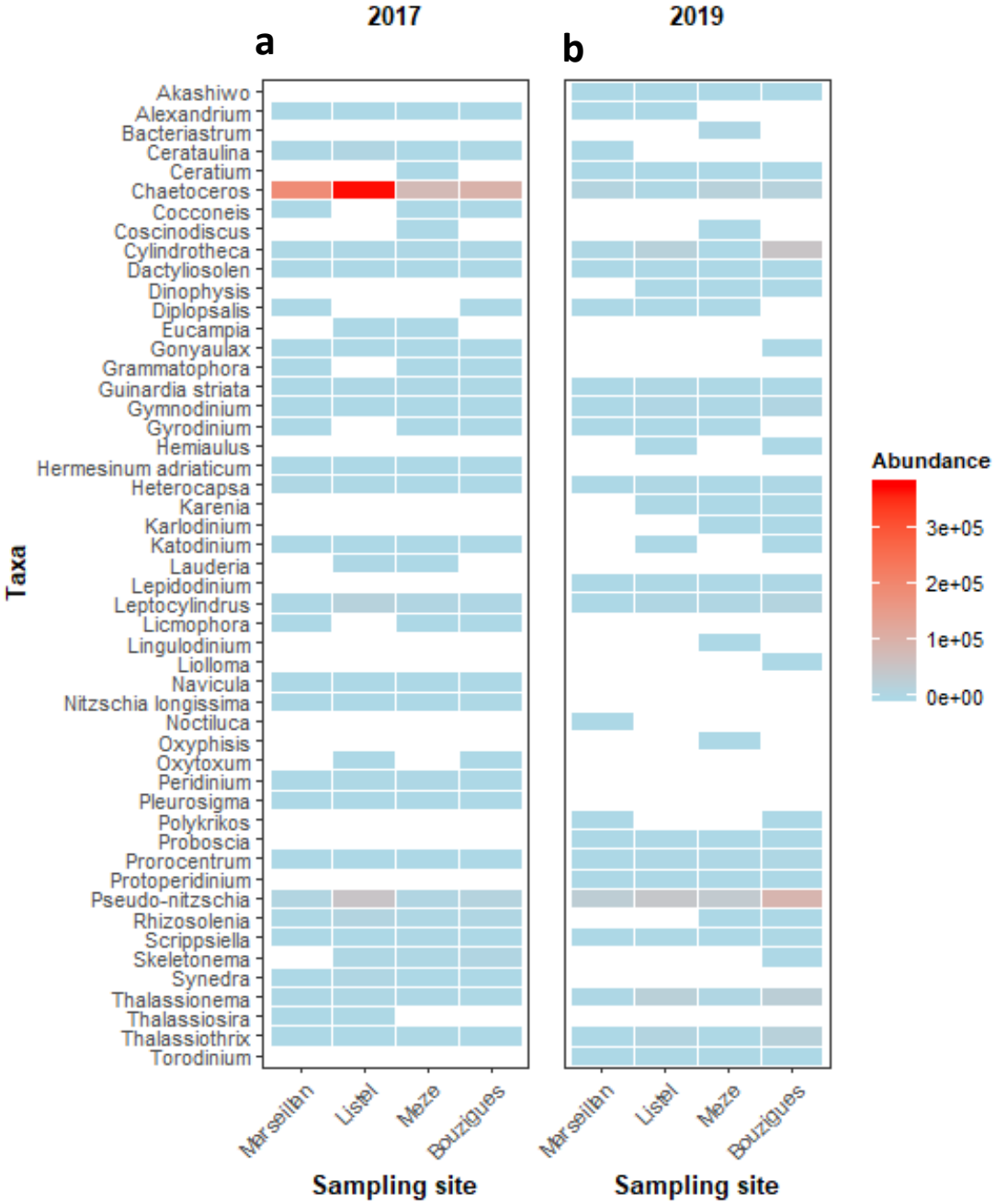

754

755 Fig. 6: Heatmap of microphytoplankton genera with changes in abundances in 2017 (no
756 heatwave) and 2019 (heatwave). Average phytoplankton abundance (cells L^{-1}) per taxon and
757 sampling site in (a) 2017 (n = 5) and (b) in 2019 (n = 4).

758

759 *Table S1: Summary of the parameters characterizing the oyster larvae analyzed in this study*

Variables	Description	Unit of measure	Abbreviation
Oyster variables			
Pediveligers	*Abundance of pre-settled pediveliger larvae on collector plates*	*ind. plate^{-1}*	*pediveligers*
Metamorphosed postlarvae	*Abundance of newly metamorphosed postlarvae on collector plates*	*ind. plate^{-1}*	*postlarvae*
Young settlers	*Abundance of pediveligers+ postlarvae on collector plates*	*ind. plate^{-1}*	*young settlers*
Juveniles	*Abundance of recruited juveniles on collector plates*	*ind. plate^{-1}*	*juveniles*
Prodissoconch II size	*Measurement of prodissoconch maximum shell height along maximal dorsoventral axis of larvae or juvenile Pacific oysters*	*µm*	*PII size*
Total fatty acids in young settlers	*Total fatty acid contents in larvae (young settlers)*	*ng lavae^{-1}*	*TFA*
Essential fatty acids	*Sum of essential fatty acids in larvae (docosahexaenoic acid (22:6ω3; DHA), eicosapentaenoic acid (20:5ω3; EPA) and arachidonic acid (AA))*	*ng lavae^{-1}*	*EFA*

760

761 *Table S2: Summary of the parameters characterizing the environment analyzed in this study.*

Variables	*Description*	*Unity*	*Abbreviation*
Environmental variables			
Temperature	*Discrete measure*	*°C*	*-*
Salinity	*Discrete measure*	*No unit*	*-*
Oxygen concentration	*Discrete measure*	*mg l^{-1}*	*-*
Total particulate matter$_{0.7\text{-}20\ \mu m}$	*Total particular pelagic material in the 0.7-20 µm fraction*	*mg l^{-1}*	*$TPM_{0.7\text{-}20\mu m}$*
Particulate organic matter$_{0.7\text{-}20\mu m}$	*Particulate pelagic material in fraction the 0.7-20 µm fraction*	*mg l^{-1}*	*$POM_{0.7\text{-}20\mu m}$*
Particulate inorganic matter$_{0.7\text{-}20\mu m}$	*Particulate inorganic pelagic material in the fraction 0.7-20 µm fraction*	*mg l^{-1}*	*$PIM_{0.7\text{-}20\mu m}$*
TFA content in $TPM_{0.7\text{-}20}$	*TFA content in $TPM_{0.7\text{-}20}$*	*µg mg $TPM_{0.7\text{-}20}^{-1}$*	
Total chlorophyll a	*Total chlorophyll a biomass*	*µgChla l^{-1}*	*Chloa*
Total chlorophyll b	*Total chlorophyll b biomass*	*µgChlb l^{-1}*	*Chlob*
Total chlorophyll c	*Total chlorophyll c biomass*	*µgChlc l^{-1}*	*Chloc*
Picophytoplankton biomass	*Chlorophyll a biomass in the <3 µm fraction (picoeukaryotes)*	*µgChla l^{-1}*	*pico_Chloa*
Nanophytoplankton biomass	*Chlorophyll a biomass in the 3-20 µm fraction (nanoeukaryotes)*	*µgChla l^{-1}*	*nano_Chloa*
Picophytoplankton+ nanophytoplankton	*Biomass*	*µgChla l^{-1}*	*nano_total_Chloa*
Microphytoplankton > 20 µm	*Biomass (microeukaryotes)*	*µgChla l^{-1}*	*micro_Chloa*
Bacteria	*Abundance of picocyanobacteria (<1 µm)*	*10^6 cell. l^{-1}*	*bacteria*
Total picoeukaryotes	*Abundance*	*10^6 cell. l^{-1}*	*peuk_tot*
picoeukaryotes+ cyanophyceae	*Abundance*	*10^6 cell. l^{-1}*	*pico_tot*
Nanophytoplankton	*Abundance*	*10^6 cell. l^{-1}*	*nano*
cryptophyceae	*Abundance*	*10^6 cell. l^{-1}*	*crypto*
Nanophytoplankton + cryptophyceae	*Abundance*	*10^6 cell. l^{-1}*	*nano_tot*
Heterotrophic flagellates	*Abundance*	*cell l^{-1}*	*HF*
Ciliates	*Abundance*	*cell l^{-1}*	*ciliates*
Tintinnidae	*Abundance*	*cell l^{-1}*	*tinti*
Diatoms	*Abundance*	*cell l^{-1}*	*diatom*
Dinoflagellates	*Abundance*	*cell l^{-1}*	*dinoflagellate*
Territorial competition by worms			
Worm coverage	*Percent cover of tubeworms (Ficopomatus enigmaticus) on plates*	*%*	*-*

762

763

Table S3: multivariate PERMANOVA investigating site and year effect for Temperature

Source	df	SS	MS	Pseudo-F	P(perm)	Unique perms	P(MC)
site	3	7,087	2,3623	1,158	0,3305	9951	0,3335
year	1	135,72	135,72	66,53	0,0001	9825	0,0001
position	1	3,2	3,2	1,5686	0,2085	9805	0,217
sitexyear	3	0,3865	0,12883	0,063154	0,9764	9951	0,9754
sitexposition	3	2,573	0,85767	0,42042	0,7357	9950	0,7371
yearxposition	1	1,1045	1,1045	0,54142	0,4681	9828	0,473
sitexyearxposition	3	0,0865	0,028833	0,014134	0,9977	9955	0,9977
Res	64	130,56	2,04				
Total	79	280,72					

Table S4: multivariate PERMANOVA investigating site, depth and year effect for salinity

Source	df	SS	MS	Pseudo-F	P(perm)	Unique perms	P(MC)
Site	3	5,331	1,777	7,5677	0,0002	9962	0,0004
Year	1	2,2445	2,2445	9,5587	0,0031	9805	0,0034
position	1	0,072	0,072	0,30663	0,5764	9733	0,5827
sitexyear	3	0,5245	0,17483	0,74457	0,5286	9960	0,5323
sitexposition	3	0,059	0,019667	0,083755	0,9666	9945	0,9679
yearxposition	1	0,1125	0,1125	0,47911	0,4824	9806	0,4966
sitexyearxposition	3	0,0805	0,026833	0,11428	0,9545	9942	0,9503
Res	64	15,028	0,23481				
Total	79	23,452					

Table S5: multivariate PERMANOVA investigating site, depth and year effect for oxygen

Source	df	SS	MS	Pseudo-F	P(perm)	Unique perms	P(MC)
site	3	3,8333	1,2778	1,3099	0,2739	9944	0,27
year	1	15,878	15,878	16,277	0,0004	9825	0,0001
position	1	10,039	10,039	10,292	0,002	9854	0,0018
sitexyear	3	10,01	3,3366	3,4205	0,0215	9947	0,0217
sitexposition	3	3,8499	1,2833	1,3156	0,2758	9955	0,2805
yearxposition	1	3,3048	3,3048	3,388	0,0708	9812	0,0682
sitexyearxposition	3	1,7959	0,59865	0,6137	0,6012	9955	0,5985
Res	64	62,43	0,97547				
Total	79	111,14					

Table S6: multivariate PERMANOVA investigating site and year effect for TPM

Source	df	SS	MS	Pseudo-F	P(perm)	Unique perms	P(MC)
site	3	1,493	0,49767	0,28089	0,8424	9962	0,8364
year	1	207,48	207,48	117,1	0,0001	9839	0,0001
sitexyear	3	2,0244	0,67479	0,38085	0,7691	9958	0,7708
Res	100	177,18	1,7718				
Total	107	388,6					

Table S7: multivariate PERMANOVA investigating site and year effect for PIM

Source	df	SS	MS	Pseudo-F	P(perm)	Unique perms	P(MC)
site	3	0,11747	0,039156	0,039431	0,9901	9949	0,9904
year	1	54,939	54,939	55,325	0,0001	9814	0,0001
sitexyear	3	0,33001	0,11	0,11077	0,957	9958	0,9508
Res	100	99,303	0,99303				
Total	107	154,73					

Table S8: multivariate PERMANOVA investigating site and year effect for POM

Source	df	SS	MS	Pseudo-F	P(perm)	Unique perms	P(MC)
site	3	1,4638	0,48793	2,796	0,0429	9952	0,0407
year	1	48,888	48,888	280,15	0,0001	9824	0,0001
sitexyear	3	1,193	0,39765	2,2787	0,0834	9952	0,0832
Res	100	17,451	0,17451				
Total	107	69,327					

Table S9: multivariate PERMANOVA investigating site, size and year effect for CHLOA

Source	df	SS	MS	Pseudo-F	P(perm)	Unique perms	P(MC)
site	3	3,35	1,1167	3,9887	0,0088	9958	0,0088
year	1	3,6519	3,6519	13,045	0,0003	9848	0,0007
taille	2	1,8257	0,91286	3,2608	0,0401	9953	0,0456
sitexyear	3	2,9083	0,96945	3,4629	0,0167	9953	0,0175
sitexsize	6	1,984	0,33066	1,1811	0,3199	9933	0,3246
yearxsize	2	5,0665	2,5333	9,0488	0,0004	9951	0,0004
sitexyearxsize	6	0,84964	0,14161	0,50582	0,8156	9949	0,8092
Res	96	26,876	0,27995				
Total	119	46,512					

Table S10: multivariate PERMANOVA investigating site and year effect for PEUK_TOT

Source	df	SS	MS	Pseudo-F	P(perm)	Unique perms	P(MC)
site	3	1,2885E+16	4,2951E+15	1,3441	0,2784	9945	0,2768
year	1	1,959E+16	1,959E+16	6,1306	0,0155	9835	0,0187
sitexyear	3	2,6684E+15	8,8948E+14	0,27835	0,8512	9952	0,8401
Res	32	1,0226E+17	3,1955E+15				
Total	39	1,374E+17					

Table S11: multivariate PERMANOVA investigating site, size and year effect for CYAN

Source	df	SS	MS	Pseudo-F	P(perm)	Unique perms	P(MC)
site	3	2,552E+16	8,5068E+15	0,7044	0,5664	9949	0,5635
year	1	5,3384E+17	5,3384E+17	44,205	0,0001	9851	0,0001
sitexyear	3	1,2146E+16	4,0486E+15	0,33524	0,8082	9953	0,797
Res	32	3,8645E+17	1,2077E+16				
Total	39	9,5796E+17					

Table S12: multivariate PERMANOVA investigating site, size and year effect for PICO

Source	df	SS	MS	Pseudo-F	P(perm)	Unique perms	P(MC)
site	3	2,3685E+15	7,8951E+14	0,083154	0,9729	9939	0,9697
year	1	7,5797E+17	7,5797E+17	79,832	0,0001	9841	0,0001
sitexyear	3	3,7254E+15	1,2418E+15	0,13079	0,9431	9944	0,938
Res	32	3,0383E+17	9,4946E+15				
Total	39	1,0679E+18					

Table S13 : multivariate PERMANOVA investigating site, size and year effect for NANO

Source	df	SS	MS	Pseudo-F	P(perm)	Unique perms	P(MC)
site	3	1,2396E+12	4,1319E+11	0,13497	0,9421	9944	0,9377
year	1	1,7765E+13	1,7765E+13	5,8032	0,0196	9837	0,0175
sitexyear	3	2,0028E+13	6,6759E+12	2,1807	0,1051	9950	0,1082
Res	32	9,7961E+13	3,0613E+12				
Total	39	1,3699E+14					

Table S14 : multivariate PERMANOVA investigating site, size and year effect for BACT_TOT

Source	df	SS	MS	Pseudo-F	P(perm)	Unique perms	P(MC)
site	3	1,622E+19	5,4066E+18	0,93657	0,4508	9949	0,4387
year	1	2,909E+20	2,909E+20	50,392	0,0001	9839	0,0001
sitexyear	3	1,0607E+19	3,5358E+18	0,61249	0,6213	9957	0,6151
Res	32	1,8473E+20	5,7728E+18				
Total	39	5,0246E+20					

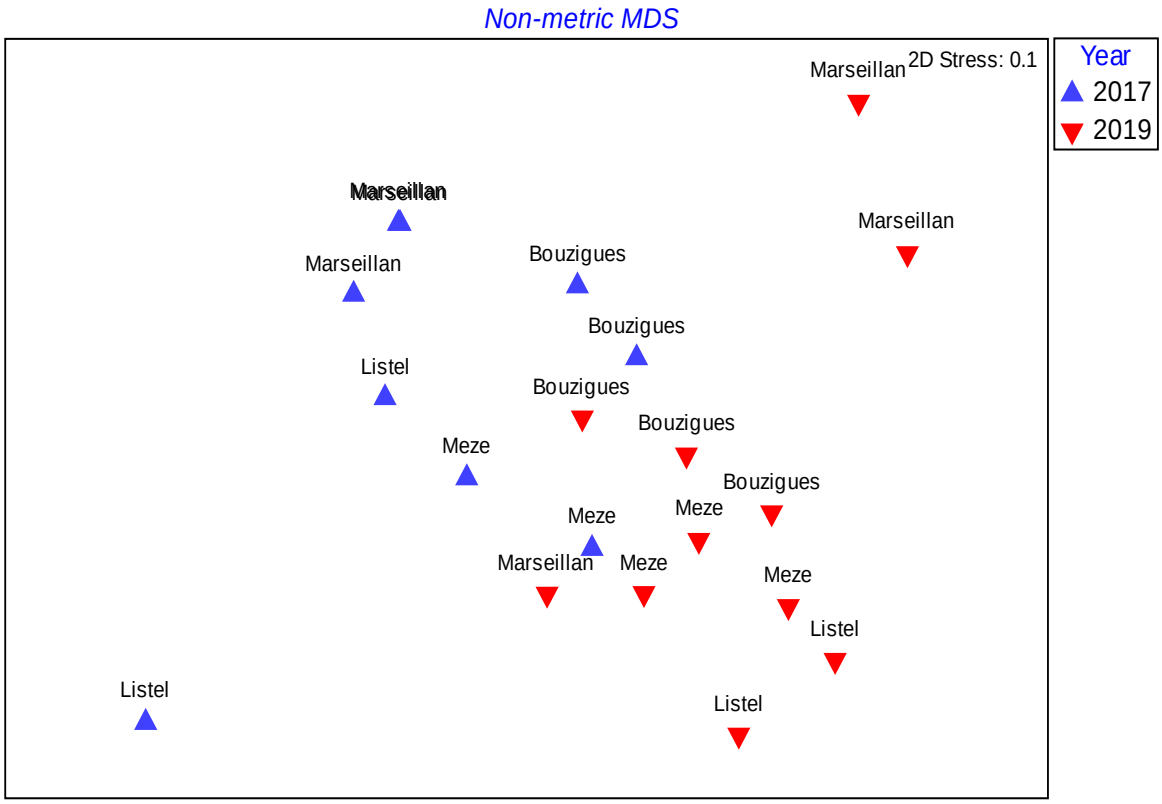

889

890 *Figure S1. Non-metric multidimensional scaling of the Euclidean similarity matrix based on the relative abundance of fatty*
891 *acid profiles measured in young settler larvae collected in 2017 and 2019 at each sampling site in the Thau lagoon.*

892

Failure of bivalve foundation species recruitment related to trophic changes during an extreme heat wave event

Alana Correia-Martins[1], Réjean Tremblay[1], Béatrice Bec[2], Cécile Roques[2], Ariane Atteia[3], Angélique Gobet[3], Marion Richard[3], Masami Hamaguchi[4], Toshihiro Miyajima[5], Masakazu Hori[4], Gilles Miron[6], Stéphane Pouvreau[7], Franck Lagarde[3*]

[1]Institut des sciences de la mer, Université du Québec à Rimouski, 310 allée des Ursulines, G5L 3A1, Rimouski, QC, Canada

[2]MARBEC, Univ Montpellier, CNRS, Ifremer, IRD, Montpellier, France

[3]MARBEC, Univ Montpellier, CNRS, Ifremer, IRD, Sète, France

[4]National Research Institute of Fisheries and Environment of Inland Sea, Fisheries Research Agency, Maruishi 2-17-5, Hatsukaichi, Hiroshima 739-0452, Japan

[5]Marine Biogeochemistry Group, Atmosphere and Ocean Research Institute, University of Tokyo, Kashiwanoha 5-1-5, Kashiwa, Chiba 277-8564, Japan

[6]Département de biologie, Université de Moncton, 18 avenue Antonine-Maillet, E1A 3E9 Moncton, NB, Canada

[7]UMR LEMAR 6539, IFREMER, Argenton-en-Landunvez, France

*Corresponding author

RUNNING PAGE HEAD: Failure of oyster recruitment during heatwave

ABSTRACT

Bivalves are regulators of coastal lagoons and provide a wide range of ecosystem services. However, coastal lagoons are sensitive to climate change. Our objective was to describe the drivers of the cascade of ecological events that occurred during a summer heatwave and resulted in recruitment failure of the Pacific oyster *Crassostrea gigas*. Results showed that elevated temperatures and salinity caused a shift in planktonic food availability toward smaller taxa. These trophic changes did not affect food accumulation by oyster larvae or their fatty acid composition but did affect post-metamorphosis success with up to 24% fewer young metamorphosed postlarvae at some sites and ~~absence~~ no development of juveniles ~~development~~ at all sites. This resulted in the failure of oyster recruitment and in the development of tubeworms, a trophic and spatial competitor that can better ingest small particles. This knowledge suggests that in the context of marine heatwaves, the ecological limits of oyster larvae are narrower than their physiological limits.

KEYWORDS

Climate change, Phenology, Extreme Heatwave, Bivalves, Pacific Oyster, *Crassostrea gigas*, Reproduction, Larval Ecology, Cascade of Environmental Effects, Trophic Changes.

1. INTRODUCTION

Coastal lagoons provide a wide range of ecosystem services (Villamagna et al. 2013, Kermagoret et al. 2019, van der Schatte Olivier et al. 2020)~~,~~ associated with biodiversity, including bivalves that are of great ecological interest and high commercial value. Bivalves also have important regulatory functions in the ecosystem thanks to their capacity to extract particles, to regenerate and store nutrients, and to form hard biogenic structures (Smaal et al. 2018). However, because coastal lagoons are shallow and exchange with the ocean is limited, they are highly sensitive to eutrophication, heatwaves, hypoxia and acidification, as well as to the effects of global climate change (Lloret et al. 2008, Lu et al. 2018, Thomas et al. 2018). An atmospheric heatwave is defined as five consecutive days with a maximum temperature 5 °C above the 1976-2005 normal (Jouzel et al. 2014). Summer 2019 was characterized by two heatwaves of exceptional intensity ~~over~~ in France, including the Thau Basin, one lasting from June 24 to July 7, the other from July 21 to 27. The absolute heat record for France (46 °C) was measured in Vérargues in the Hc~~é~~rault administrative department (Météo-France 2019), which includes the Thau ~~basin~~Basin. A 13-day period of temperature stress between June 24 and July 13 was recorded with water temperatures above 27.5 °C in the Thau lagoon (Lagarde et al. 2021, Messiaen et al. 2021). Marine heatwaves (MHW) are extreme events defined as abrupt but prolonged periods of high sea surface temperatures that can occur anywhere, at any time (Scannell et al. 2016, Schlegel et al. 2017, Hobday et al. 2018). More specifically, an abnormally warm event is considered to be a MHW if it lasts for five or more days, with temperatures higher than the 90th percentile based on a 30-year historical baseline period (Hobday et al. 2016). High water temperatures increase the metabolic requirements of bivalves (Filgueira et al. 2016, Thomas & Bacher 2018). Even if temperatures remain within the species' thermal range, high

temperatures combined with variations in salinity and/or food availability ~~variations~~, can negatively impact the life cycle of bivalves (Filgueira et al. 2016, Scanes et al. 2020, Vázquez et al. 2021).

The development of planktonic larvae of the Pacific oyster (*Crassostrea gigas*) underlies their complex life history strategy (Byrne & Przeslawski 2013, Ko et al. 2014, Dineshram et al. 2016). The context of hydroclimatic stress~~ors~~ provides a range of environmental possibilities that need to be described in order to better understand the larvae development ~~of larvae~~. Several studies suggest that global changes are disrupting plankton communities and their nutritional values by affecting the abundance, size and diversity of primary producers (Klauschies et al. 2012, Sommer et al. 2012, Trombetta et al. 2019). Generally, elevated temperatures affect phytoplankton cell size with a shift from larger to smaller species (Bec et al. 2005, Trombetta et al. 2019). Adult bivalves can assimilate small phytoplanktonic particles (Sonier et al. 2016). However, the efficiency of ~~the~~ capture is regulated by the morphology of their gills, and efficiency is generally low when small particles such as picoplankton are present (Rosa et al. 2018). Larvae feed through a less selective velum (Bower & Meyer 1990). Marine phytoplankton species are major producers of long-chain polyunsaturated essential fatty acids (EFA) but are now predicted to decrease due to ocean warming (Hixson & Arts 2016, Colombo et al. 2017). The fatty acids docosahexaenoic acid (22:6ω3; DHA), eicosapentaenoic acid (20:5ω3; EPA) and arachidonic acid (AA) are essential for the growth and survival of marine invertebrates, particularly during their metamorphosis from pelagic larvae to benthic juveniles and ultimately, their recruitment success (Gagné et al. 2010, Bassim et al. 2015). Since EFAs are poorly biosynthesized by marine animals, their intake

depends on their food (Glencross 2009, Da Costa et al. 2015). Thus, both the right size of larval food and the right fatty acid composition are essential for the recruitment success of bivalves. The aim of this study was to identify the environmental factors and trophic conditions (Table S1 & Table S2) associated with the recruitment failure of the Pacific oyster, *Crassostrea gigas*, during a heat wave. We compared two contrasted years (2017, ~~when there was~~ no heatwave and 2019, ~~when~~ occurrence of a heatwave ~~occurred~~) ~~in~~ at four sites in the Thau lagoon, France (Fig. 1). We hypothesize that heatwaves, characterized by high temperatures and high salinity, have a negative impact on oyster recruitment due to poor larval feeding conditions caused by changes in plankton diversity.

2. MATERIALS AND METHODS

2.1 Experimental design

Annual oyster recruitment was monitored at four experimental sites in the Thau lagoon (~~southern~~ Southern France; Fig 1.) on the same dates, i.e. between July 24 and August 21, in 2017, and between July 2 and July 29, in 2019. The average depth of the Thau lagoon is 4 m, and the lagoon covers an area of 7 500 ha (19 km x 4.5 km) of which 20% is used for shellfish culture (oysters and mussels). The lagoon is connected to the Mediterranean Sea via a network of channels through Sète Harbor (Fiandrino et al. 2017). Two experimental sites were located inside the shellfish farming areas (Marseillan and Bouzigues) and the other two ~~others~~ outside the shellfish farming areas (Meze and Listel) (Fig 1.).

2.2 Oyster analyses

Three sets of oyster collectors were submerged vertically 2 m below the surface at each of the four study sites in the Thau lagoon. Three different oyster settler stages (Table S1) were used to estimate benthic abundances: i) pre-settled pediveliger larvae, ii) young metamorphosed postlarvae and iii) juveniles (Arakawa 1990, Lagarde et al. 2017). The sums of abundances of pediveligers and postlarvae are listed under "young settlers" (Table S1). The collectors were installed once the oyster's larval supply reached a density of 10 000 larvae/m^3 (Pouvreau et al. 2021). The collectors located inside the shellfish culture areas were suspended from existing farming structures. Those outside the area were suspended using a tailored mooring system (Lagarde et al. 2017, 2019). Each collector was made of 44 white PVC plastic plates (15 cm in diameter; surface area 250 cm^2) stacked on a 110 cm long tube. Two weeks after their immersion, three plates per collector were harvested [at the top (i.e., the 5^{th} from the top of the collector), in the middle (the 22^{nd}) and at the bottom (the 39^{th})] and data were pooled to assess the abundance of young settlers and fatty acid (FA) content (µg $larva^{-1}$). A similar sampling procedure was used four weeks after the collectors were immersed to assess the abundance of juveniles.

The abundance of young settlers and juveniles was assessed on the upper surface of each plate using standard 15 cm^2 sub-units. Depending on ~~the~~ abundance, 3 to 12 sub-units were randomly selected for counting and the resulting replicates were averaged to obtain the total number of individuals per plate. Recruitment was evaluated from the abundance of juveniles and metamorphosis from the ratio of juvenile to young-settler abundances. Size at metamorphosis was estimated by measuring the prodissoconch II (PII) (Martel et al. 1995). M~~A m~~aximum ~~of~~ 60 juveniles were removed from each plate sampled after the fourth week after immersion, and placed on a plasticine flange fixed on a microscope blade. Observations were made under the

wide-range zoom lens of a high-resolution digital microscope Keyence (VHX 2000E, 1 µm resolution, HDR images), and the maximum dorsoventral axis was measured. This measurement corresponds to the distance between the umbo and the most distant part of the clear demarcation formed by a growth line delimiting the PII from the dissoconch shell.

The fatty acid (FA) composition of young settlers was determined using a pool of 77 to 212 individuals per replicate (2-3 replicates per site depending on pediveliger abundances). Samples were preserved in vials filled with 3 mL of dichloromethane methanol (CH_2Cl_2:MeOH, 2:1 v:v), closed with a Teflon-lined cap under nitrogen atmosphere and stored at -80 °C until analysis. Lipids were extracted by grinding in dichloromethane methanol using a modified Folch procedure (Parrish 1999). Fatty acid methyl esters (FAME) were prepared using sulfuric acid and methanol (2:98 v:v) heated at 100 °C for 10 min and using 19:0 as internal standard (Lepage & Roy 1984). Samples were purified on an activated silica gel with 1 mL of hexane ethyl acetate (v:v) to eliminate free sterols. FAME were analyzed in the full scan mode (ionic range: 50–650 m:z) on a Polaris Q ion trap coupled ~~to~~ with a Trace GC Ultra gas chromatograph (Thermo Scientific) equipped with a TriPlus autosampler, a PTV injector and an ITQ900 mass detector (Thermo Scientific). An Omegawax 250 (Supelco) capillary column was used for separation using high purity helium. Xcalibur v.2.1 software (Thermo Scientific) was used for FAME identification and quantification with the standard reference solution (Supelco 37 Component FAME Mix and Supelco menhaden oil). Unknown peaks were identified according to their mass spectra with emphasis on FA trophic makers.

2.3 Environmental measurements

Environmental factors were measured once a week (Table S1 and Table S2) starting just after ~~immersion of~~ the collectors were immersed and continuing until all the plates were harvested, i.e., a total of five weeks. Temperature (°C), salinity and dissolved oxygen concentrations (mg L^{-1}) were measured at a depth of 1 m and at the bottom of the water column with an Oxi1970i WTW oximeter and an LF 197-S WTW conductivity meter.

Potential food for oysters is expressed as the concentration of total suspended particulate matter varying in size from 0.7 and 20 µm ($TPM_{0.7\text{-}20\mu m}$, mg L^{-1}). It consisted of inorganic ($PIM_{0.7\text{-}20\mu m}$, mg L^{-1}) and organic particulate matter ($POM_{0.7\text{-}20\mu m}$, mg L^{-1}). Once a week, three replicate water samples were collected at a depth of 1 m using a Ruttner Standard Water Sampler (Hydro-Bios Apparatebau) and stored at 4 °C for less than 2 hours before filtration ~~for~~ to ~~the~~ measure~~ment of~~ the concentrations (mg mL^{-1}) of pico and nano-seston. In 2017, 500-mL subsamples of 1-L samples were used for filtration, while on 2019, 1-L subsamples of 2-L samples were used ~~in 2019~~. Water samples were first filtered by gravity through a Nuclepore membrane (20 µm pore size). Fractionated water samples were then filtered using a vacuum pressure pump (0.3 bar) on pre-weighed (Mettler Toledo XP6 microbalance) pre-combusted (at 500 °C) Whatman 25 mm GF/F filters (0.7 µm pore size). The GF/F filters were rinsed with an isotonic seawater solution of ammonium formate (38 g L^{-1} distilled water) to eliminate salt deposits and stored in Millipore™ PetriSlide™ containers at – 25 °C. The filters were dried at 70 °C for 24 h, weighed and the concentration of total particulate matter $TPM_{0.7\text{-}20\mu m}$ was determined. The filters were then combusted at 500 °C for 5 h and weighed again to determine the concentration of particulate inorganic matter ($PIM_{0.7\text{-}20\mu m}$, mg L^{-1}). The concentration of particulate organic

matter ($POM_{0.7\text{-}20\mu m}$, mg L^{-1}) ~~was~~ is the difference in weight between the dried and the combusted filter. To determine the FA content of the pico- and nano-seston (µg.mg $TPM_{0.7\text{-}20\mu m}^{-1}$), 1-L water samples collected in 2017 and 2-L water samples collected in 2019 were filtered as described above without addition of ammonium formate solution. GF/F filters were stored in 3 ml of CH_2Cl_2:MeOH (2:1 v:v) under a nitrogen atmosphere in vials closed with a Teflon-lined cap and stored at -80 °C. The mass of total fatty acids in the seston (MTFA; µg mg^{-1} POM) and its composition (% fatty acids) were obtained as already described for oysters, with lipid extraction carried out by sonification rather than grinding.

Plankton diversity was ~~collected~~ measured in 1 -L samples collected in 2017 and in 2 -L samples collected weekly in 2019 ~~collected weekly~~ with a Ruttner Standard Water Sampler (Hydro-Bios Apparatebau) at each sampling site. This sampling strategy enabled 40 observations (4 sites x 5 weeks x 2 years). Phytoplankton was characterized using the standard Utermöhl method NF-EN-152014, 2006 in 10 mL seawater samples. Abundances of 52 diatom taxa and 38 dinoflagellate taxa are expressed as the number of individuals per liter. Chlorophyll *a* (Chl-*a*), *b* (Chl-*b*) and *c* (Chl-*c*) biomasses were evaluated in 200 ml seawater samples filtered ~~(Bec et al. 2005, 2011)~~ on Whatman GF/F membranes (0.7 µm pore size) with a vacuum pressure pump (<10 cm Hg) (Bec et al. 2005, 2011). Filters were stored in glass tubes at -20 °C until analysis. To determine the contribution of picophytoplankton (<3 µm), nanophytoplankton (3 to 20 µm) and microphytoplankton (>20 µm), two out of three samples were size-fractioned beforehand by gravity through Nuclepore membranes (3 and 20 µm pore size). Filters were ground in acetone (90%) and extracted at 4 °C for 24 h in the dark. Pigment contents were measured with a spectrofluorometer (Perkin-Elmer LS50b) (Neveux & Lantoine 1993) and are expressed in

µg ~~chl~~Chl *a* L^{-1}. Concentrations of picocyanobacteria (<1 µm), autotrophic picoeukaryotes (<3 µm), nanophytoplankton (3-20 µm) and bacteria were estimated using a FACSCalibur flow cytometer according to ~~Becton Dickinson~~flow cytometry methods (Marie et al. 1997, Bec et al. 2011). Seawater samples (1-ml) were analyzed; abundances are expressed in cells per liter. Total picophytoplankton abundances were assessed by summing picocyanobacteria and photosynthetic picoeukaryote abundances. Fluorescent beads (0.94 µm; 2 and 3 µm, Polysciences) were added to each sample to calibrate for cell size of phytoplankton in terms of equivalent spherical diameter. To measure bacterial abundances, seawater samples were fixed with prefiltered (0.2 µm) buffered formaldehyde (2% final concentration) and stored in liquid nitrogen. The procedure was slightly modified as higher concentrations of fluorochromes (SYBR Green I) were used (Bouvy et al. 2016). The fixed samples were incubated with SYBR Green I (Molecular Probes) at a final concentration of 1/375 at 4 °C for 15 min in the dark. Stained bacterial cells excited at 488 nm were determined according to their side-scattered light and green fluorescence collected using a 530/ 30 nm filter. Fluorescent beads (0.94 µm; Polysciences) were added to each sample as size reference beads.

Protozooplankton (heterotrophic flagellates) abundances were determined using the standard 2006 Utermöhl method NF-EN-152014, and are expressed in cells per liter. Until used for heterotrophic flagellate analysis, 30 -ml seawater samples were preserved with 2.5 -ml of prefiltered (0.2 µm) formaldehyde and kept at 4 °C in the dark. Before counting, 10 ml subsamples were stained with 4',6-diamidino-2-phenylindole (DAPI) to reach a final concentration of 2.5 µg ml^{-1}. Heterotrophic flagellates were counted by size class (2-5 µm, 5-10 µm and >10 µm) under an epifluorescence microscope (Olympus AX70) with UV illumination (Sherr et al. 1993).

2.4 Territorial competition

The percent cover of tubeworms (*Ficopomatus enigmaticus*) on 6 plates per site sampled in the fourth week after immersion was estimated to assess territorial competition with oyster juveniles, but only during the 2019 sampling season, as no tubeworms were observed in 2017. In 2017, each plate used for oyster sampling was checked for the presence of potential competitors, which ~~is~~ was when the absence tubeworms was ~~observed~~noted. Photographs of each plate were taken ~~of each plate~~ with a GoPro HERO4 Silver camera equipped with a macro pro filter (San Mateo, CA, USA) and in 2019, the % of tubeworms recovered on the plate was estimated using Image-Pro Insight 9.1 software (MediaCybernetics, Rockville, MD, USA).

2.5 Statistical analyses

All PERMANOVA analyses were performed with Primer 7 and Permanova+1 (version 7.0.13) software. A two-way PERMANOVA (n perm.: 9999) was conducted using a Euclidian distance matrix to test the effect of year (2 fixed levels) and sampling site (4 fixed levels) on size at metamorphosis, total and essential fatty acid contents in young settlers, and on all the environmental variables measured, except the oxygen level, which was added as a third factor (depth) in the analysis. Homogeneity was evaluated using the permutation analysis of multivariate dispersion (PERMDISP)~~ routine~~. When significant PERMANOVAs were observed, post hoc multiple comparison tests were carried out. Multivariate analyses of total FA composition in young settlers and in seston, including *a posteriori* pairwise comparison, were done using distance-based permutational multivariate analysis of variance (PERMANOVA, 9999 permutations) based on Euclidian dissimilarities, with year (2 fixed

levels) and sampling site (4 fixed levels) as sources of variation. Variations in FA composition, expressed in percentages, were visualized using non-metric multidimensional scaling (n-MDS). The similarity percentage (SIMPER) procedure was performed on untransformed data to identify the FAs that explained the most dissimilarity between significantly different levels.

3. RESULTS

3.1 Oyster recruitment

Recruitment numbers showed dramatic annual variability with great success at some sites in 2017 but an overall near-zero recruitment level at all sites in 2019 (Fig. 2a, b). In 2017, the metamorphosis survival rate, expressed as the ratio of juvenile to young settler abundances per plate, also showed marked spatial variability (Fig. 2a). The ratio of juvenile (123 ± 9 ind. plate^{-1}) to young-settler abundances per plate (49 ± 6 ind. plate^{-1}) was 2.5 in Bouzigues. However, at the other sites, the level of recruitment was 24% lower (94 ± 16 juveniles plate^{-1}) in Meze, 90% (13 ± 2 juveniles plate^{-1}) in Listel, and 97% (4 ± 2 juveniles plate^{-1}) in Marseillan. A ~~lower~~smaller supply of larvae (6 ± 2 young-settlers plate^{-1}) was observed in Marseillan, but the metamorphosis survival rate was 0.6. However, in Meze and Listel, the low recruitment rates were not linked to the supply of larvae, as young settler abundances were higher in Meze (328 ± 71 young settler plate^{-1}, with a metamorphosis survival rate of 0.3) and in Listel (670 ± 65 young settler plate^{-1}, with a metamorphosis survival rate of 0.02) than in Bouzigues. Failure characterized the 2019 oyster recruitment season: low abundances of young settlers were observed in Meze (116 ± 5 ind. plate^{-1}) and in Listel (31 ± 2 ind. plate^{-1}), with almost 3 and 22 times fewer individuals than in 2017, respectively. This trend was not observed in Bouzigues (84 ± 9 ind. plate^{-1}) or in Marseillan (45 ± 3 ind. plate^{-1}) in 2019. Instead, young settlers were

267 respectively 2 and 7 times higher in 2019 than in 2017. However, two weeks later, almost no
268 juveniles were observed on the plates (average 0.14 ± 0.06 ind. plate^{-1}), regardless of the sites,
269 pointing to a general oyster recruitment failure in 2019.
270 The size of the juveniles at metamorphosis (PII length) was established in all samples~~,~~ except
271 in samples from Bouzigues in 2019 (Fig 2c, d), in which no metamorphosis of young settlers to
272 juveniles was observed. PII individuals sampled in 2019 were 5.1% smaller (mean 262 ± 1 µm)
273 than those sampled in 2017 (mean 276 ± 1 µm). Differences among sites were only observed in
274 2017, when PII sizes in Bouzigues were 2.7% smaller than those in Meze ($p = 0.02$), Listel (p
275 $= 0.01$) and Marseillan ($p = 0.03$).
276 No significant differences in total fatty acid (TFA) contents were observed in young settlers ~~in~~
277 at the four sites and in the two years ($p > 0.05$). The overall TFA average was 51 ± 19 ng larvae^{-}
278 ^{1}. The sum of essential fatty acids (EFA) corresponded to about 10% of TFA with an effect of
279 year × site (pseudo-$F_{3,19}$=6.47, p=0.007), as individuals in Listel (p=0.02) and Marseillan
280 (p=0.006) had 5 times lower EFA contents in 2017 than in 2019. The fatty acid composition of
281 young settlers varied with the year × site interaction (pseudo-$F_{3,19}$=2.34, p=0.017), as
282 individuals sampled in Listel (p=0.047) and Marseillan (p=0.044) had different profiles ~~in~~
283 between the two years (Fig. S1). According to a SIMPER analysis, the interannual
284 differences observed at these two sites were linked to DHA (22:6n3), EPA (20:5n3), AA
285 (20:4n6), 18:2n6, 18:0 and 16:0 explained more than 83% of the average dissimilarity in the
286 fatty acid profiles. DHA, EPA and AA levels in young settlers sampled in 2019 were twice
287 higher than in 2017, while the levels of 18:2n6 were five times lower in 2019 than in 2017,
288 except ~~for~~ at the Meze and Bouzigues sites ($p > 0.09$).
289

3.2 Physico-chemical parameters

Average water temperatures were 2.6 ºC higher in 2019 than in 2017, respectively, 26.8 °C (withthe maximum temperature measured at the surface in Marseillan, (August 7, 2019, with 29.7 °C) and 24.2 °C. In the same way, salinity was 0.3 higher, respectively, 39.3 and 39.0, respectively, in 2019 than in 2017 (Fig 3a, b, Table S3 and Table S4). A site effect was also observed for salinity in the Thau lagoon. On average over the 2 years, observed salinity increased from east to west: mean salinity (39.5) in Marseillan was 0.68 higher than in Bouzigues where mean salinity was 38.8. Conversely, no significant difference in temperature was observed among sites although the averages varied from 23.8 °C in Bouzigues to 24.5 °C in Marseillan in 2017 and from 26.3 °C to 27.2 °C, respectively, in 2019. There was an interaction site × year interaction effect on the oxygen concentration (Table S5). No significant difference was observed among sites in 2017 with oxygen concentrations ranging between 6.23 mg O_2 l^{-1} and 6.53 mg O_2 l^{-1} (Fig. 3c). The lowest mean oxygen concentration, 5.64 mg O_2 l^{-1} at the surface of the lagoon and 3.52 mg O_2 l^{-1} at the bottom, were observed in Bouzigues in 2019 (p = 0.001) during the heatwave (p = 0.001). Oxygen concentrations varied with water depth, lower values were generally observed near the bottom (Fig. 3c). Minimum concentrations of oxygen, i.e. below 2mg l^{-1}, were recorded as early as July 8, 2019 at the bottom of the lagoon in Bouzigues.

3.3 Potential food for oyster larvae

Concentrations of $TPM_{0.7\text{-}20}$, $PIM_{0.7\text{-}20}$and $POM_{0.7\text{-}20}$ were more than twice higher in 2019 than in 2017 (Fig. Fig. 4a, b, c, Table S6, S7 and S8). Significant differences among the four sites were only observed in the concentrations of $POM_{0.7\text{-}20}$ concentrations. In For both years,

Code de champ modifié

Mis en forme : Police :12 pt

313 $POM_{0.7\text{-}20}$ concentrations in Marseillan were 0.7 and 0.8 times lower than in Listel and Meze
314 ($p = 0.01$ and 0.03, respectively). An effect of the year × ~~chl~~Chl-*a* biomass~~es~~ fraction was
315 observed (Table S9). Mean nanophytoplankton and picophytoplankton biomasses ($p = 0.0001$
316 and $p = 0.0004$ respectively) were 3 times higher in 2019 ~~(Fig.4d, e)~~ than in 2017 (Fig.4d, e). A
317 site × year effect was also observed, ~~chl~~Chl-*a* biomass values were 45% lower in Bouzigues
318 than in Listel ($p=0.01$) and Meze ($p = 0.004$) in 2017. In 2019, biomass~~es~~ in Marseillan was~~ere~~
319 62% lower than at the other sites ($p < 0.02$). Interannual variability in ~~chl~~Chl-*a* biomass ~~was~~
320 ~~found~~ in Bouzigues was found to be ~~with~~ 3 times ~~more biomass~~ in 2019 ($p = 0.0007$) than in
321 2017. Similar patterns were observed for ~~chl~~Chl-*b* and ~~chl~~Chl -*c* biomass, with twice as much
322 ~~chl~~Chl-*b* in the samples collected in 2019 than in the samples collected in 2017 (0.069 µg L^{-1}
323 versus 0.026 µg L^{-1}; $p=0.0001$), and a more than two-fold increase in ~~chl~~Chl-*c* (0.103 ug L^{-1}
324 versus 0.046 ug L^{-1}), particularly in Listel ($p=0.039$) and Bouzigues ($p=0.0003$).
325 Oysters feed primarily on nanophytoplankton and microphytoplankton based on diatoms and
326 dinoflagellates, both of which decreased in 2019 relative to 2017 in favor of picoplankton. Flow
327 cytometry data showed an effect of the year on cells smaller than 3 µm (Fig. ~~Fig. 5~~). Abundances
328 of picoeukaryotes (< 3 µm) (Table S10), picocyanobacteria (< 1 µm) (Table S11 and S12) and
329 bacteria (Table S14) were higher in 2019 than in 2017. However, nanophytoplankton (3-20 µm)
330 abundances decreased by 39% in 2019 (Table S13). The abundance of total heterotrophic
331 flagellates did not vary significantly among sites or between years, the mean value being~~:~~ 2 866
332 ± 291 cell mL^{-1}. Dinoflagellate and diatom abundances were affected by the year (pseudo-
333 $F_{1,35}$=5.64, p=0.023), total values decreased by 60% in 2019 compared to 2017. These variations
334 were linked to a 93% decrease in *Chaetoceros* abundance from 184 715 ± 66 846 to 12 483 ± 3
335 540 cells L^{-1} (SIMPER contribution: 77%, pseudo-$F_{1,35}$=8.73, p=0.0001) and ~~a decrease that led~~

Mis en forme : Police :12 pt

~~to~~ the disappearance of *Skeletonema* in Listel and Meze between 2017 and 2019. Diatom taxa were fewer in number at all sites sampled in 2019 with a maximum of 13 identified compared to 21 taxa identified in 2017. A marked increase in *Pseudo-nitzschia* (19 920 ± 10 513 to 50 562 ± 13 652 cells L^{-1}) with a SIMPER contribution of 8% and (pseudo-$F_{1,35}$=8.73, p=0.0001), *Leptocylindrus* (SIMPER contribution 7%), *Thalassionema,* and *Cylindrotheca* (1 837 ± 222 to 18 712 ± 12 010 cells L^{-1}) was observed in 2019 compared to 2017. This trend was particularly ~~apparent~~ clear in Bouzigues (Fig. 6). This result also reflects the higher diversity of dinoflagellate taxa observed in 2019 (16 taxa) than in 2017 (12 taxa).

TFA contents in the $TPM_{0.7\text{-}20}$ samples were twice higher in 2019 (19.2 µg mg $TPM_{0.7\text{-}20}^{-1}$) than in 2017 (9.9 µg mg $TPM_{0.7\text{-}20}^{-1}$;pseudo-$F_{1,61}$=17.1, p=0.0002) with no differences among sites and year × site effects. The fatty acid composition of the $TPM_{0.7\text{-}20}$ samples differed between years (pseudo-$F_{3,76}$=3.08, p=0.0001) and, as determined by SIMPER analysis, explained 97% of the differences in the levels of 18:1n9, 18:0, 16:1, 18:2n6, 16:0, 14:0, 20:5n3 and 22:6n3. Twenty-six percent of the difference observed between years was related to 18:1n9, an FA that was twice as abundant in 2017 (up to 24.1% of the TFA) ~~compared to~~than in 2019. The dissimilarity in the FA profiles observed between years was also explained by higher values of 18:2n6 (representing up to 10.8% of TFA), and EPA (7%) in 2017. 18:2n6 and EPA were, respectively, 11.3% and 5% higher in 2017 than in 2019. The most abundant FAs in the $TPM_{0.7\text{-}20}$ samples in 2019 were 16:1 and DHA, which explained, respectively, 13% and 4.3% of the dissimilarity revealed by SIMPER analysis.

3.4 Territorial competition by worms

The percent cover of tubeworms (*Ficopomatus enigmaticus*) on the plates in 2019 showed a marked increase in this species. Differences were observed among the sites (pseudo-$F_{3,33}$=157, p=0.0001). Results showed a similar percent cover of tubeworms (93.6 ± 1.5%) in Listel and Bouzigues and a lower percent cover in Meze (83.2 ± 2.6%) ($p < 0.032$) and in Marseillan (23.6 ± 3.7%) ($p < 0.0001$).

4. DISCUSSION

The aim of this study was to identify the environmental and trophic drivers of the decline in the recruitment of the Pacific oyster, *Crassostrea gigas*, associated with a heatwave. Our hypothesis that a heatwave has a negative effect on oyster recruitment by altering plankton diversity is supported by our results. The year 2017 is a reference year from a hydroclimatic point of view with known ecological functioning of larval development of oysters (Lagarde et al. 2017, 2019). The larval developments led to different metamorphosis rates in the study areas that are linked to environmental cues such as the abundance of nanophytoplankton (Lagarde et al. 2017, 2018). If there are more spat than larvae, we assume 100% successful metamorphosis by competent larvae and the arrival of competent larvae from elsewhere between the two observation periods, i.e. between the 14th and 28th day after the collectors were installed (Lagarde et al. 2017). While oyster recruitment was normal in 2017, an unprecedented failure was observed in summer 2019 in the Mediterranean Thau lagoon. The atmospheric conditions that prevail during a heatwave have strong direct effects on marine and lagoon environments that normally provide a variety of ecosystem services and host valuable ~~host~~ species (Sarà et al. 2021). Temperature and salinity conditions are key ecological and physiological factors for *Crassostrea* larvae (His et al. 1989b,

Baldwin & Newell 1995, Devakie & Ali 2000, Troost et al. 2009). In controlled experimental ~~settings~~conditions, the entire larval life of *C. gigas*, including metamorphosis, showed high tolerance to temperatures ranging from 17 °C to 32 °C at a salinity level of 34, with low mortality (≤10%) and a maximum growth rate at 32 °C (Rico-Villa et al. 2009). The physiological limits of temperature tolerance were therefore not reached in our experimental conditions where the average temperature was 26.8 °C during the heatwave (with a maximum of with 29.7 °C measured at the surface of the lagoon in Marseillan~~,~~ on August 7, 2019), so in this case, temperature was not the origin of the failure ~~in this case~~. Salinity did not drop below 38 in ~~either the~~ 2017 ~~or~~ and 2019 recruitment season, and intermittently reached more than 40 in 2019. *Crassostrea gigas* is an estuarine organism that tolerates a wide range of salinity (Nell & Holliday 1988), but no information is available in the literature on the upper salinity tolerance of the larval stage in real conditions. The high salinity in 2019 may represent the physiological salinity threshold for oyster larvae. Our results showed that ~~the larval shell (prodissoconch)~~ at the time of metamorphosis (PII), the larval shell (prodissoconch) was smaller in 2019, suggesting a reduction in larval growth or more rapid achievement of metamorphosis competence in high salinity years. ~~In agreement with Nell and Holliday (1988), who reported an~~ An optimal salinity range for larval growth up to 27 and very marked reduction in growth has been observed at 31-39 ~~(Nell & Holliday 1988),~~ (Nell & Holliday 1988). ~~the~~ The smaller observed PII size could be ~~related~~ linked to growth limitation under high salinity. Interestingly, ~~Nell & Holliday reported~~ no significant effect of salinity on larval survival between 19 and 39 has been reported, but a marked reduction in larval growth rate has been observed from 30 ~~on was reported by?~~ (Helm & Millican 1977, Nell & Holliday 1988). The upper tolerance limits of oysters to high salinity ranging from 35 to 45 should thus be further tested in ~~the~~ laboratory

conditions, including interactions between high temperatures and different nutritional inputs (His et al. 1989a).

Marine bivalve populations are known to be unstable due to causes intrinsic to the population or to extrinsic causes linked to environmental conditions (Skazina et al. 2013, Reed et al. 2021). The heatwave that occurred in 2019 resulted in large quantities of particulate matter and chlorophyll biomass, but their quality appeared to be unfavorable for oyster recruitment. The failure of oyster recruitment in 2019 could thus be linked to the change in ~~the~~ phytoplankton ~~community~~ communities with low abundance of forage diatoms and high abundance of picoplanktonic prokaryotes and eukaryotes, of heterotrophic flagellates, ~~and~~ as well as of the diatoms *Pseudo-Nitzschia* and *Cylindrotheca*. However, the trophic environment was not characterized by a planktonic community poor in fatty acids, ~~and it was~~ in fact it was richer than in 2017. Pediveliger larvae accumulated the same quantity of fatty acids in ~~2019~~ 2017 as in ~~2017~~2019, but metamorphosis failures were observed at all sites. We suggest that this failure may be linked to inappropriate trophic conditions, due to the development of picophytoplankton~~which in turn, are mainly linked to the size of picoplankton species~~. These species are poorly retained by the newly developed gills of postlarvae. Our results suggest that the overabundance of small particles (picoplanktonic prokaryotes and eukaryotes) could be critical for larval settlement and metamorphosis. Higher chlorophyll biomass was observed in the nanophytoplankton fraction during the heatwave in 2019 than in 2017 (with no heatwave), indicating changes in the phytoplankton community.

The heat wave was characterized by the ~~Increasing~~ increasing abundances of picocyanobacteria (Bec et al. 2005, Collos et al. 2009, Derolez et al. 2020b) and decreasing abundances of nanophytoplankton. The oligotrophication trajectory of the Thau lagoon began in the early

2000s (Collos et al. 2009, Derolez et al. 2020a). This process caused a community shift due to a reduction in nutrient loads that had prevailed since the 1970s thanks to improved wastewater treatment in the watershed aimed at halting eutrophication (EC 1991a b, 2000). The reduction in nutrient loads has been amplified by a decrease in total rainfall since the 2000s due to climate change (Derolez et al. 2020a). Our results corroborate evidence that the proportion of small taxa, like picoplankton, in the phytoplankton community, is increasing in coastal, marine and freshwater ecosystems in response to global warming (Daufresne et al. 2009, Mousing et al. 2014, Pinckney et al. 2015). Small phytoplankton cells have been reported to dominate in oligotrophic environments (Irwin et al. 2006).

The 2019 heatwave had a negative impact on oyster larval recruitment by shifting the phytoplankton community towards picoplankton and opening a favorable ecological window for tubeworms that compete for food and land space. In this case, the failure of recruitment seems to be more linked to the ecological conditions at the time of metamorphosis of the larvae than to their physiological limits, which were not reached. We hypothesize that the limitations encountered by oyster larvae are ecological in the sense of the absence of trophic settlement triggers (Toupoint et al. 2012, Androuin et al. 2022), which are known to be ~~the~~ high concentrations of diatoms and high abundance of nanophytoplankton for metamorphosis survival in the Thau Lagoon (Lagarde et al. 2017, 2018). Tubeworms are opportunistic ecosystem engineers that play an important role in determining benthic species abundance and composition (Heiman & Micheli 2010, McQuaid & Griffiths 2014). In our case, high temperatures and high salinity coincided with the development of the tubeworm *Ficopomatus enigmaticus,* triggering a shift in benthic community composition that was destructive for oyster

recruitment on collectors. The feeding abilities of *F. enigmatus* make it very efficient for small particles, with high ingestion rates in the size range 2-16 µm, including diatoms (Davies et al. 1989, Bruschetti et al. 2008), which exert strong top-down trophic control (Pan & Marcoval 2014). We consequently hypothesize that tubeworms are important territorial competitors and trophic competitors of oyster larvae in shallow water and brackish habitats that develop in the context of heatwaves.

This study demonstrates, for the first time, an ecological process leading to the recruitment failure of the Pacific oysters due to an extreme heatwave. The oligotrophication trajectory of our study site combined with the effects of high water temperatures caused ~~variations in~~a shift of ~~the~~ phytoplankton communities ~~that benefit~~towards small species of picophytoplankton including cyanobacteria, but that are likely unfavorable for the successful larval development of oysters until their juvenile metamorphosis (Lagarde et al. 2017). The present study thus reveals the ecological limits of the recruitment process of the Pacific oyster in the context of a heatwave in a Mediterranean lagoon. The heatwave phenomenon observed in 2019 severely disrupted the reproductive cycle of oysters in the Thau lagoon. In this context, the oyster nursery function in an oyster farming ecosystem~~,~~ can only be achieved or maintained when pico-, nano- and microphytoplankton communities are present and abundant and oysters can find favorable areas for larval development and optimize their recruitment. This study provides evidence that, in the conditions ~~brought about~~created by a heatwave, the ecological limits of Pacific oyster larvae are narrower than their physiological limits. The effects of climate change, particularly the warming of waters in semi-enclosed basins, will certainly lead to problems in larval harvesting in the near future~~s~~. The i~~I~~nformation ~~presented~~ included in this paper should help adapt oyster aquaculture, including husbandry practices, to a future marked by climate change.

5. Data and code availability

All the data used in the current study and the scripts used in our analysis are publicly available or were obtained by the corresponding author. This research benefited from the VELYGER Database: The Oyster Larvae Monitoring French Project (http://doi.org/10.17882/41888) and REPHY Dataset - French Observation and Monitoring program for Phytoplankton and Hydrology in coastal waters. Metropolitan data. SEANOE (https://doi.org/10.17882/47248).

6. REFERENCES

Androuin T, Barbier P, Forêt M, Meziane T, Thomas M, Archambault P, Winkler G, Tremblay R, Olivier F (2022) Pull the trigger: interplay between benthic and pelagic cues driving the early recruitment of a natural bivalve assemblage. Ecosphere 13:e03672.

Arakawa KY (1990) Natural Spat Collecting in the Pacific Oyster *Crassostrea gigas* (Thunberg). Mar Behav Physiol 17:95–128.

Baldwin BS, Newell RI (1995) Feeding rate responses of oyster larvae (*Crassostrea virginica*) to seston quantity and composition. J Exp Mar Bio Ecol 189:77–91.

Bassim S, Chapman RW, Tanguy A, Moraga D, Tremblay R (2015) Predicting growth and mortality of bivalve larvae using gene expression and supervised machine learning. Comp Biochem Physiol - Part D Genomics Proteomics 16:59–72.

Bec B, Collos Y, Souchu P, Vaquer A, Lautier J, Fiandrino A, Benau L, Orsoni V, Laugier T (2011) Distribution of picophytoplankton and nanophytoplankton along an anthropogenic eutrophication gradient in French Mediterranean coastal lagoons. Aquat Microb Ecol 63:29–45.

Bec B, Husseini-Ratrema J, Collos Y, Souchu P, Vaquer A (2005) Phytoplankton seasonal

495 dynamics in a Mediterranean coastal lagoon: Emphasis on the picoeukaryote community.
496 J Plankton Res 27:881–894.
497 Bouvy M, Got P, Domaizon I, Pagano M, Leboulanger C, Bouvier C, Carre C, Roques C, Dupuy
498 C (2016) Plankton communities in the five Iles Eparses (Western Indian Ocean) considered
499 to be pristine ecosystems. Acta oecologica- Int J Ecol 72:9–20.
500 Bower SM, Meyer SG (1990) Atlas of anatomy and histology of larvae and early juvenile stages
501 of Japanese scallop *Patinopecten yessoensis*. Can Spec Publ Fish Aquat Sci 111:1–51.
502 Bruschetti M, Luppi T, Fanjul E, Rosenthal A, Iribarne O (2008) Grazing effect of the invasive
503 reef-forming polychaete Ficopomatus enigmaticus (Fauvel) on phytoplankton biomass in
504 a South West Atlantic coastal lagoon. J Exp Mar Bio Ecol 354:212–219.
505 Byrne M, Przeslawski R (2013) Multistressor impacts of warming and acidification of the ocean
506 on marine invertebrates' life histories. Integr Comp Biol 53:582–596.
507 Collos Y, Bec BB, Jauzein C, Abadie E, Laugier T, Lautier J, Pastoureaud A, Souchu P, Vaquer
508 A (2009) Oligotrophication and emergence of picocyanobacteria and a toxic dinoflagellate
509 in Thau lagoon, southern France. J Sea Res 61:68–75.
510 Colombo SM, Wacker A, Parrish CC, Kainz MJ, Arts MT (2017) A fundamental dichotomy in
511 long-chain polyunsaturated fatty acid abundance between and within marine and terrestrial
512 ecosystems. Environ Rev 25:163–174.
513 Da Costa F, Robert R, Quéré C, Wikfors GH, Soudant P (2015) Essential fatty acid assimilation
514 and synthesis in larvae of the bivalve *Crassostrea gigas*. Lipids 50:503–511.
515 Daufresne M, Lengfellner K, Sommer U (2009) Global warming benefits the small in aquatic
516 ecosystems. Proc Natl Acad Sci 106:12788 LP – 12793.
517 Davies BR, Stuart V, de Villiers M (1989) The filtration activity of a serpulid polychaete

518 population *Ficopomatus enigmaticus* (Fauvel) and its effects on water quality in a coastal
519 marina. Estuar Coast Shelf Sci 29:613–620.
520 Derolez V, Malet N, Fiandrino A, Lagarde F, Richard M, Ouisse V, Bec B, Aliaume C (2020a)
521 Fifty years of ecological changes: Regime shifts and drivers in a coastal Mediterranean
522 lagoon during oligotrophication. Sci Total Environ 732:139292.
523 Derolez V, Soudant S, Malet N, Chiantella C, Richard M, Abadie E, Aliaume C, Bec B (2020b)
524 Two decades of oligotrophication: evidence for a phytoplankton community shift in the
525 coastal lagoon of Thau (Mediterranean Sea, France). Estuar Coast Shelf Sci:106810.
526 Devakie MN, Ali AB (2000) Salinity-temperature and nutritional effects on the setting rate of
527 larvae of the tropical oyster, *Crassostrea iredalei* (Faustino). Aquaculture 184:105–114.
528 Dineshram R, Chandramouli K, Ko GWK, Zhang H, Qian PY, Ravasi T, Thiyagarajan V (2016)
529 Quantitative analysis of oyster larval proteome provides new insights into the effects of
530 multiple climate change stressors. Glob Chang Biol 22:2054–2068.
531 EC (1991a) Council Directive 91/271/EEC concerning urban waste-water treatment. Official
532 Journal L 135, 30.5.1991, p. 40–52.
533 EC (1991b) Council Directive 91/676/EEC of 12 December 1991 concerning the protection of
534 waters against pollution caused by nitrates from agricultural sources. Official Journal L
535 375 , 31/12/1991 P. 0001 - 0008.
536 EC (2000) Directive 200/60/EC of the european parliament and of the council of 23 october
537 2000 establishing a framework for community action in the field of water policy.
538 Fiandrino A, Ouisse V, Dumas F, Lagarde F, Pete R, Malet N, Le Noc S, de Wit R (2017)
539 Spatial patterns in coastal lagoons related to the hydrodynamics of seawater intrusion. Mar
540 Pollut Bull 119:132–144.

541 Filgueira R, Guyondet T, Comeau LA, Tremblay R (2016) Bivalve aquaculture-environment
542 interactions in the context of climate change. Glob Chang Biol 22:3901–3913.
543 Gagné R, Tremblay R, Pernet F, Miner P, Samain JF, Olivier F (2010) Lipid requirements of
544 the scallop *Pecten maximus* (L.) during larval and post-larval development in relation to
545 addition of *Rhodomonas salina* in diet. Aquaculture 309:212–221.
546 Glencross BD (2009) Exploring the nutritional demand for essential fatty acids by aquaculture
547 species. 71–124.
548 Heiman KW, Micheli F (2010) Non-native Ecosystem Engineer Alters Estuarine Communities.
549 Integr Comp Biol 50:226–236.
550 Helm MM, Millican PF (1977) Experiments in the hatchery rearing of Pacific oyster larvae.
551 Aquaculture 11:1–12.
552 His E, Robert R, Dinet A (1989a) Combined effect of temperature and salinity on fed and
553 starved larvae of the Mediterranean mussel *Mytilus galloprovincialis* and the Japanese
554 oyster *Crassostrea gigas*. Mar Biol 100:455–463.
555 His E, Robert R, Dinet A (1989b) Marine biology of the Mediterranean mussel *Mytilus*
556 *galloprovincialis* and the Japanese oyster *Crassostrea gigas*. Mar Biol 100:455–463.
557 Hixson SM, Arts MT (2016) Climate warming is predicted to reduce omega-3, long-chain,
558 polyunsaturated fatty acid production in phytoplankton. Glob Chang Biol 22:2744–2755.
559 Hobday AJ, Alexander L V., Perkins SE, Smale DA, Straub SC, Oliver ECJ, Benthuysen JA,
560 Burrows MT, Donat MG, Feng M, Holbrook NJ, Moore PJ, Scannell HA, Sen Gupta A,
561 Wernberg T (2016) A hierarchical approach to defining marine heatwaves. Prog Oceanogr
562 141:227–238.
563 Hobday AJ, Oliver ECJ, Gupta A Sen, Benthuysen JA, Burrows MT, Donat MG, Holbrook NJ,

564 Moore PJ, Thomsen MS, Wernberg T, Smale DA (2018) Categorizing and naming marine
565 heatwaves. Oceanography 31:162–173.
566 Irwin AJ, Finkel Z V., Schofield OME, Falkowski PG (2006) Scaling-up from nutrient
567 physiology to the size-structure of phytoplankton communities. J Plankton Res 28:459–
568 471.
569 Jouzel J, Ouzeau G, Déqué M, Jouini M, Planton S, Vautard R (2014) Le climat de la France au
570 XXIe siècle (Volume 4), Scénarios régionalisés: édition 2014 pour la métropole et les
571 régions d'outre-mer.
572 Kermagoret C, Claudet J, Derolez V, Nugues MM, Ouisse V, Quillien N, Baulaz Y, Le Mao P,
573 Scemama P, Vaschalde D, Bailly D, Mongruel R (2019) How does eutrophication impact
574 bundles of ecosystem services in multiple coastal habitats using state-and-transition
575 models. Ocean Coast Manag 174:144–153.
576 Klauschies T, Bauer B, Aberle-Malzahn N, Sommer U, Gaedke U (2012) Climate change
577 effects on phytoplankton depend on cell size and food web structure. Mar Biol 159:2455–
578 2478.
579 Ko GWK, Dineshram R, Campanati C, Chan VBS, Havenhand J, Thiyagarajan V (2014)
580 Interactive Effects of Ocean Acidification, Elevated Temperature, and Reduced Salinity
581 on Early-Life Stages of the Pacific Oyster. Environ Sci Technol 48:10079–10088.
582 Lagarde F, Atteia Van Lis A, Gobet A, Richard M, Behzad M, Roques C, Foucault E, Messiaen
583 G, Hubert C, Cimiterra N, Derolez V, Bec B (2021) Phénomène d'Eaux Vertes à
584 *Picochlorum* en lagune de Thau pendant les années 2018 et 2019. Observations
585 environnementales. FRANCE.
586 Lagarde F, Fiandrino A, Ubertini M, Roque d'Orbcastel E, Mortreux S, Chiantella C, Bec B,

Mis en forme : Français (France)

Mis en forme : Français (France)

587 Bonnet D, Roques C, Bernard I, Richard M, Guyondet T, Pouvreau S, Lett C (2019)
588 Duality of trophic supply and hydrodynamic connectivity drives spatial patterns of Pacific
589 oyster recruitment. Mar Ecol Prog Ser 632:81–100.
590 Lagarde F, Richard M, Bec B, Roques C, Mortreux S, Bernard I, Chiantella C, Messiaen G,
591 Nadalini J-BB, Hori M, Hamaguchi M, Pouvreau S, Roque d'Orbcastel E, Tremblay R
592 (2018) Trophic environments influence size at metamorphosis and recruitment
593 performance of the Pacific oyster. Mar Ecol Prog Ser 602:135–153.
594 Lagarde F, Roque E, Ubertini M, Mortreux S, Bernard I, Fiandrino A, Chiantella C, Bec B,
595 Roques C, Bonnet D, Miron G, Richard M, Pouvreau S, Lett C (2017) Recruitment of the
596 Pacific oyster *Crassostrea gigas* in a shellfish-exploited Mediterranean lagoon : discovery,
597 driving factors and a favorable environmental window. Mar Ecol Prog Ser 578:1–17.
598 Lepage G, Roy CC (1984) Improved recovery of fatty acid through direct transesterification
599 without prior extraction or purification. J Lipid Res 25:1391–1396.
600 Lloret J, Marín A, Marín-Guirao L (2008) Is coastal lagoon eutrophication likely to be
601 aggravated by global climate change? Estuar Coast Shelf Sci 78:403–412.
602 Lu Y, Yuan J, Lu X, Su C, Zhang Y, Wang C, Cao X, Li Q, Su J, Ittekkot V, Garbutt RA, Bush
603 S, Fletcher S, Wagey T, Kachur A, Sweijd N (2018) Major threats of pollution and climate
604 change to global coastal ecosystems and enhanced management for sustainability. Environ
605 Pollut 239:670–680.
606 Marie D, Partensky F, Jacquet S, Vaulot D (1997) Enumeration and cell cycle analysis of natural
607 populations of marine picoplankton by flow cytometry using the nucleic acid stain SYBR
608 Green I. Appl Environ Microbiol 63:186–193.
609 Martel A, Hynes TMT, Buckland-Nicks J (1995) Prodissoconch morphology, planktonic shell

610 growth, and site at metamorphosis in *Dreissena polymorpha*. Can J Zool 73:1835–1844.
611 McQuaid KA, Griffiths CL (2014) Alien reef-building polychaete drives long-term changes in
612 invertebrate biomass and diversity in a small, urban estuary. Estuar Coast Shelf Sci
613 138:101–106.
614 Messiaen G, Mortreux S, Le Gall P, Crottier A, Lagarde F (2021) Marine environmental station
615 database of Thau lagoon.
616 Météo-France (2019) 46,0 °C à Vérargues : nouveau record officiel de température observée en
617 France. http://www.meteofrance.fr/actualites/74345599-c-est-officiel-on-a-atteint-les-46-
618 c-en-france-en-juin
619 Mousing EA, Ellegaard M, Richardson K (2014) Global patterns in phytoplankton community
620 size Structure-evidence for a direct temperature effect. Mar Ecol Prog Ser 497:25–38.
621 Nell JA, Holliday JE (1988) Effects of salinity on the growth and survival of Sydney rock oyster
622 (*Saccostrea commercialis*) and Pacific oyster (*Crassostrea gigas*) larvae and spat.
623 Aquaculture 68:39–44.
624 Neveux J, Lantoine F (1993) Spectrofluorometric assay of chlorophylls and phaeopigments
625 using the least squares approximation technique. Deep Res Part I 40:1747–1765.
626 Pan J, Marcoval MA (2014) Top-down effects of an exotic serpulid polychaete on natural
627 plankton assemblage of estuarine and brackish systems in the south west atlantic. J Coast
628 Res 30:1226–1235.
629 Parrish CC (1999) Determination of total lipid, lipid classes, and fatty acids in aquatic samples.
630 Lipids Freshw Ecosyst:4–20.
631 Pinckney JL, Benitez-Nelson CR, Thunell RC, Muller-Karger F, Lorenzoni L, Troccoli L,
632 Varela R (2015) Phytoplankton community structure and depth distribution changes in the

Mis en forme : Français (France)

633 Cariaco Basin between 1996 and 2010. Deep Sea Res Part I Oceanogr Res Pap 101:27–37.
634 Pouvreau S, Maurer D, Auby I, Lagarde F, Le Gall P, Cochet H, Bouquet A-L, Geay A, Mille
635 D (2021) VELYGER Database: The Oyster Larvae Monitoring French Project.
636 Reed AJ, Godbold JA, Solan M, Grange LJ (2021) Reproductive traits and population dynamics
637 of benthic invertebrates indicate episodic recruitment patterns across an Arctic polar front.
638 Ecol Evol 11:6900–6912.
639 Rico-Villa B, Pouvreau S, Robert R (2009) Influence of food density and temperature on
640 ingestion, growth and settlement of Pacific oyster larvae, *Crassostrea gigas*. Aquaculture
641 287:395–401.
642 Rosa M, Ward JE, Shumway SE (2018) Selective Capture and Ingestion of Particles by
643 Suspension-Feeding Bivalve Molluscs: A Review. J Shellfish Res 37:727–746.
644 Sarà G, Giommi C, Giacoletti A, Conti E, Mulder C, Mangano MC (2021) Multiple climate-
645 driven cascading ecosystem effects after the loss of a foundation species. Sci Total Environ
646 770:144749.
647 Scanes E, Parker LM, O'Connor WA, Dove MC, Ross PM (2020) Heatwaves alter survival of
648 the Sydney rock oyster, Saccostrea glomerata. Mar Pollut Bull 158:111389.
649 Scannell HA, Pershing AJ, Alexander MA, Thomas AC, Mills KE (2016) Frequency of marine
650 heatwaves in the North Atlantic and North Pacific since 1950. Geophys Res Lett 43:2069–
651 2076.
652 van der Schatte Olivier A, Jones L, Vay L Le, Christie M, Wilson J, Malham SK (2020) A
653 global review of the ecosystem services provided by bivalve aquaculture. Rev Aquac 12:3–
654 25.
655 Schlegel RW, Oliver ECJ, Wernberg T, Smit AJ (2017) Nearshore and offshore co-occurrence

656 of marine heatwaves and cold-spells. Prog Oceanogr 151:189–205.
657 Sherr EB, Caron DA, Sherr BF (1993) Staining of heterotrophic protists for visualization via
658 epifluorescence microscopy. In: *Handbook of Methods in Aquatic Microbial Ecology*, 1st
659 Editio. Kemp PF, Sherr BF, Sherr EB, Cole JJ (eds) Lewis Publishers, p 213–227
660 Skazina M, Sofronova E, Khaitov V (2013) Paving the way for the new generations: *Astarte*
661 *borealis* population dynamics in the White Sea. Hydrobiologia 706:35–49.
662 Smaal AC, Ferreira JG, Grant J, Petersen JK, Strand Ø (2018) Goods and services of marine
663 bivalves, Springer O. Cham, Switzerland.
664 Sommer U, Adrian R, Bauer B, Winder M (2012) The response of temperate aquatic ecosystems
665 to global warming: novel insights from a multidisciplinary project. Mar Biol 159:2367–
666 2377.
667 Sonier R, Filgueira R, Guyondet T, Tremblay R, Olivier F, Meziane T, Starr M, LeBlanc AR,
668 Comeau LA (2016) Picophytoplankton contribution to *Mytilus edulis* growth in an
669 intensive culture environment. Mar Biol 163:1–15.
670 Thomas Y, Bacher C (2018) Assessing the sensitivity of bivalve populations to global warming
671 using an individual-based modelling approach. Glob Chang Biol:1–18.
672 Thomas Y, Cassou C, Gernez P, Pouvreau S (2018) Oysters as sentinels of climate variability
673 and climate change in coastal ecosystems. Environ Res Lett 13:104009.
674 Toupoint N, Gilmore-Solomon L, Bourque FFF, Myrand B, Pernet F, Olivier FFF, Tremblay
675 RRR, Gilmore-Solomon L, Bourque FFF, Myrand B, Pernet F, Olivier FFF, Tremblay
676 RRR, Mohit V, Linossier I, Bourgougnon N, Myrand B, Olivier FFF, Lovejoy C, Tremblay
677 RRR, Gilmore-Solomon L, Bourque FFF, Myrand B, Pernet F, Olivier FFF, Tremblay
678 RRR (2012) Match/mismatch between the Mytilus edulis larval supply and seston quality:

679 Effect on recruitment. Ecology 93:1922–1934.
680 Trombetta T, Vidussi F, Mas S, Parin D, Simier M, Mostajir B (2019) Water temperature drives
681 phytoplankton blooms in coastal waters. PLoS One 14:1–28.
682 Troost K, Gelderman E, Kamermans P, Smaal AC, Wolff WJ (2009) Effects of an increasing
683 filter feeder stock on larval abundance in the Oosterschelde estuary (SW Netherlands). J
684 Sea Res 61:153–164.
685 Vázquez E, Woodin SA, Wethey DS, Peteiro LG, Olabarria C (2021) Reproduction Under
686 Stress: Acute Effect of Low Salinities and Heat Waves on Reproductive Cycle of Four
687 Ecologically and Commercially Important Bivalves. Front Mar Sci 8:1–19.
688 Villamagna AM, Angermeier PL, Bennett EM (2013) Capacity, pressure, demand, and flow: A
689 conceptual framework for analyzing ecosystem service provision and delivery. Ecol
690 Complex 15:114–121.
691

692 ## 7. ACKNOWLEDGEMENTS

693 The authors are grateful to the three reviewers who kindly and constructively reviewed our
694 manuscript. This research was supported by the Natural Sciences and Engineering Research
695 Council of Canada (NSERC-Discovery Grant no.299100) to R.T and by the *Ressources*
696 *Aquatiques Québec* Research Network (*Fonds de Recherche du Québec-Nature et*
697 *Technologies*, #2014-RS-171172) and MITACS (FR37656) for the internships of ACM during
698 her stay at IFREMER. This research was also funded by the VELYGER network. F.L. and R.T.
699 thank the RECHAGLO international research group, co-funded by Ifremer and the Department
700 of Fisheries and Oceans (DFO), and the *Institut France-Québec pour la coopération scientifique*

en appui au secteur Maritime (IFQM) for encouragement, support, and exchanges with Canada. F.L., M.H. T.M. and M.H. thank FREA, JSPS and Campus France/Ministry of Foreign Affairs for funding the scientific exchange needed for this study and the development of all the ideas presented by our group.

We thank Hélène Cochet, Serge Mortreux, Anaïs Crottier, Grégory Messiaen, Clarisse Hubert, Nabila Guenineche, Gabriel Devique, Hervé Violette, Elise Hatey, Camille Gianaroli and Nathalie Gauthier for logistic support in the field and technical contributions in the laboratory.

8. AUTHOR CONTRIBUTIONS

A.C.M. was involved in investigation, methodology, writing, data curation, formal analysis, and visualization. R.T. and F.L. were involved in conceptualization, funding acquisition, investigation, methodology, writing, data curation, formal analysis, visualization, and project administration. S.P. was involved in conceptualization, funding acquisition, investigation, methodology, writing and project administration. B.B was involved in conceptualization, funding acquisition, investigation, methodology, writing, data curation, formal analysis, and visualization. C.R. contributed to funding acquisition, methodology, writing, data curation and formal analysis. A.A and A.G. contributed to writing and interpretation. G.M. contributed to funding acquisition, investigation, methodology, writing and formal analysis. M.R., M.Ho, M.Ha. and T.M. contributed to conceptualization, investigation, methodology and writing.

9. COMPETING INTERESTS

The authors ~~declare~~ have no competing interests to declare.

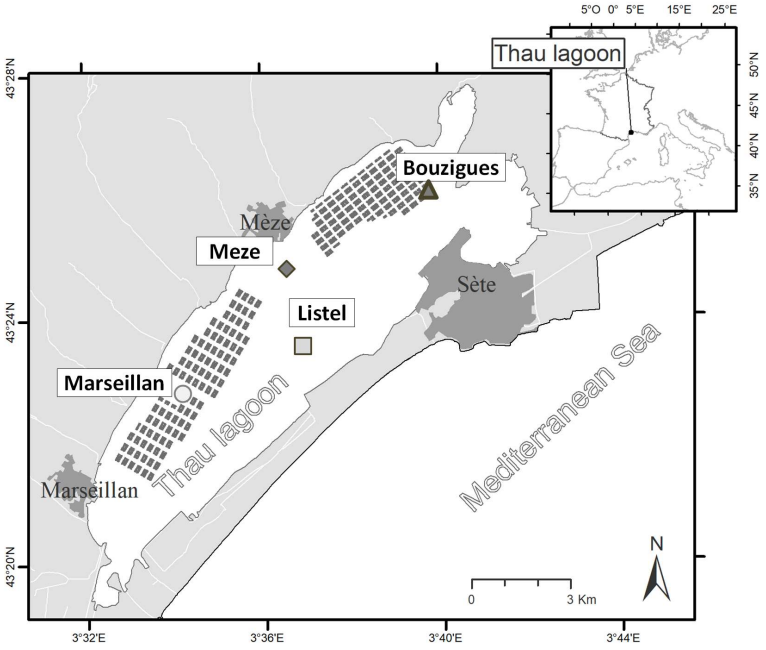

Fig. 1. The four sampling sites in the Thau lagoon. Marseillan and Bouzigues are located in the shellfish farming area; shaded areas indicate the location of shellfish culture areas. Meze and Listel are located outside the shellfish farming ~~aquaculture~~ area.

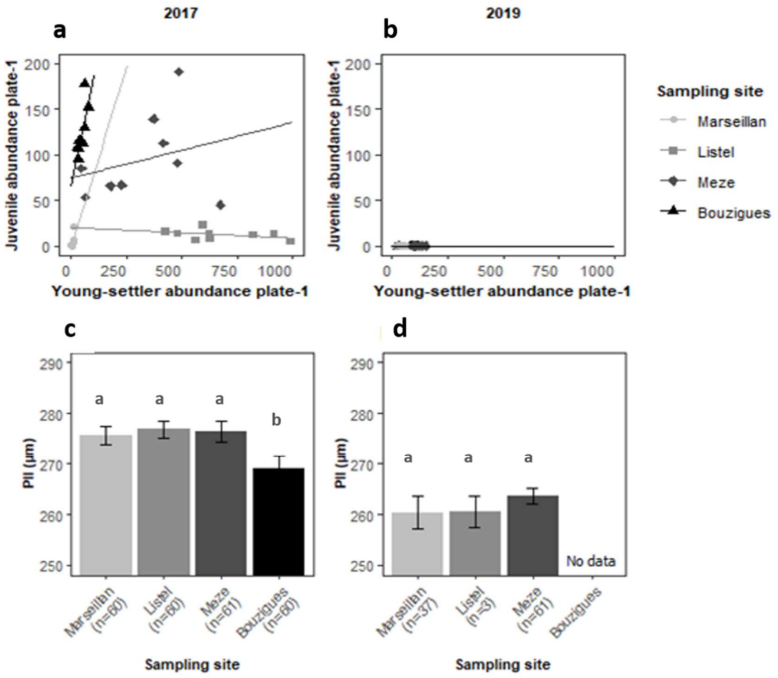

Fig. 2. Variability of oyster recruitment and prodissoconch II size ~~according to the years~~in 2017 (no heatwave) and 2019 (heatwave). *Crassostrea gigas* recruitment performance with young settlers (pediveligers + post-larvae) and juvenile abundance per collector plate observed at the four sampling sites during the summer recruitment events in (a) 2017 and in (b) 2019. Size at metamorphosis was estimated based on the length of prodissoconch II shell (PII, µm ± SE) of juveniles sampled in (c) 2017 and (d) 2019. Different letters indicate significant differences between sites according to post-hoc multiple comparison tests after PERMANOVA.

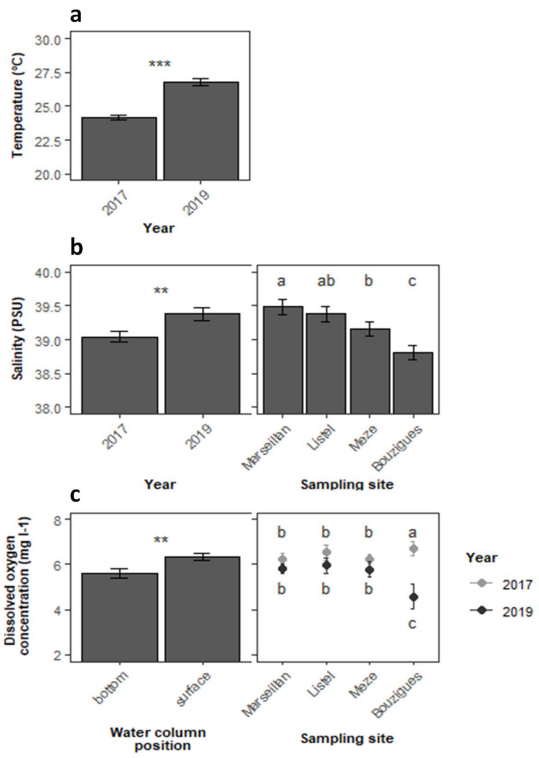

Fig. 3. Physico-chemical monitoring in 2017 (no heatwave) and 2019 (heatwave). (a) Mean temperature (°C ± SE) per year (n = 40), (b) mean salinity (PSU ± SE) per year (n = 40) and per sampling site (n = 20) and (c) mean dissolved oxygen concentration (mg L^{-1} ± SE) according to the position of the sample in the water column (n = 40) and per year and sampling site (n = 10). Asterisks indicate significant differences in average parameters per year (* $p \leq 0.05$, ** $p \leq 0.01$, *** $p \leq 0.001$). Different letters indicate significant differences between sites according to post hoc multiple comparison tests after PERMANOVA.

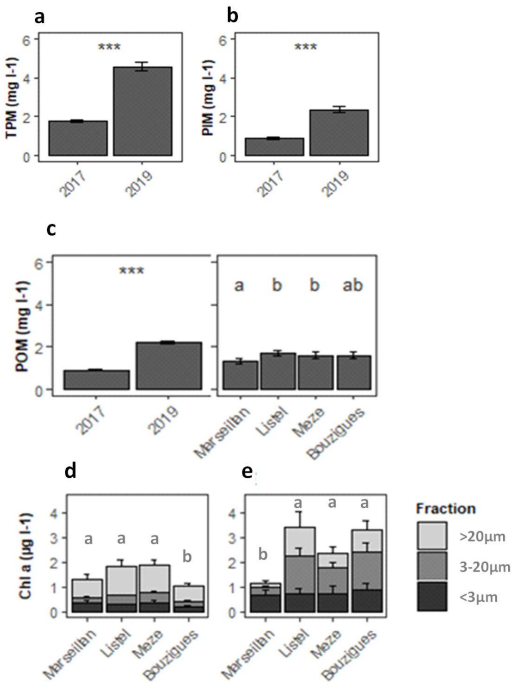

Fig. 4. Hydrobiological monitoring in 2017 (no heatwave) and 2019 (heatwave). Mean concentrations of (a) total particulate matter (TPM, mg L^{-1} ± SE), (b) particulate inorganic matter (PIM, mg L^{-1} ± SE) and (c) particulate organic matter (POM, mg L^{-1} ± SE) per year and sampling site (n = 5 per sampling site and year). Mean concentrations of chlorophyll-a (d, 2017 and e; 2019; µg L^{-1} ± SE), found in the picophytoplankton fraction (< 3 µm), the nanophytoplankton fraction (3 to 20 µm) and the microphytoplankton fraction (> 20 µm) per year and sampling site (n = 5 per sampling site, year and phytoplankton fraction). Asterisks indicate significant differences according to the average parameters per year (* $p \leq 0.05$, ** $p \leq 0.01$, *** $p \leq 0.001$). Different letters indicate significant differences between sites according to post-hoc multiple comparison tests after PERMANOVA.

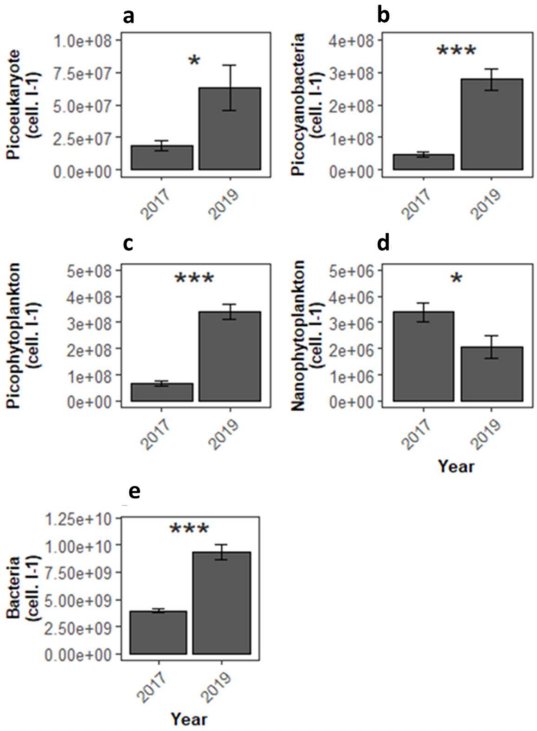

Fig. 5: Monitoring of picophytoplankton population in 2017 (no heatwave) and 2019 (heatwave). Average abundances for all sites of (a) photosynthetic picoeukaryotes, (b) picocyanobacteria, (c) picophytoplankton, (d) nanophytoplankton and (e) bacteria (cells L^{-1} ± SE) per year (n=20). Asterisks indicate significant differences according to the average parameters per year (* $p \leq 0.05$, ** $p \leq 0.01$, *** $p \leq 0.001$).

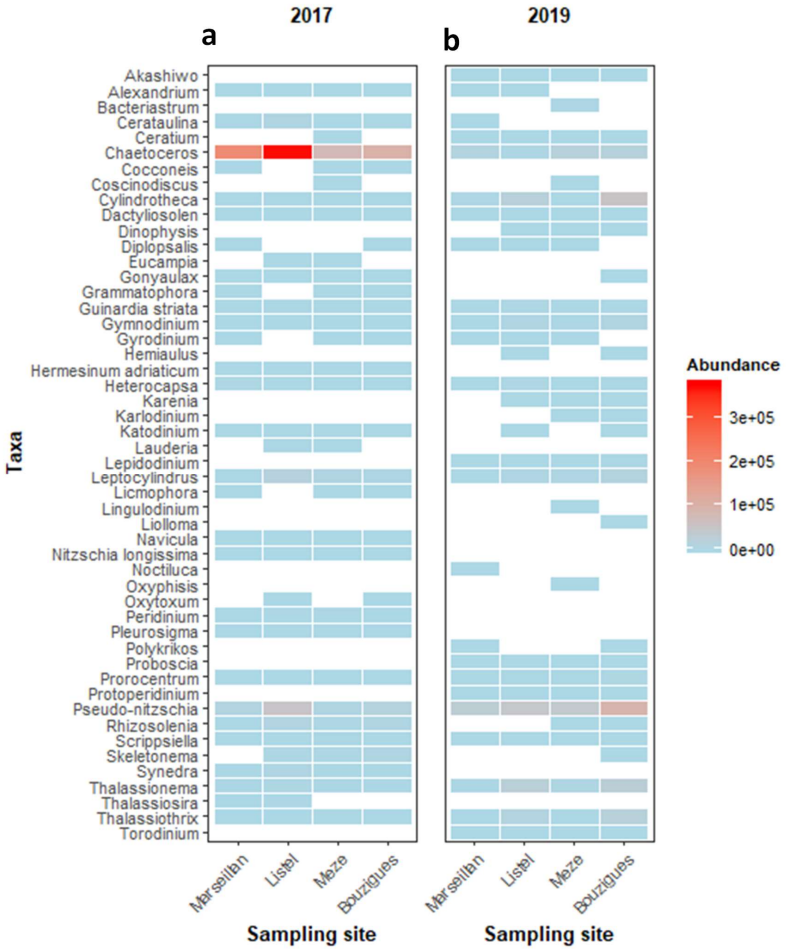

764

765 Fig. 6: Heatmap of microphytoplankton genera with changes in abundances in 2017 (no
766 heatwave) and 2019 (heatwave). Average phytoplankton abundance (cells L^{-1}) per taxon and
767 sampling site in (a) 2017 (n = 5) and (b) in 2019 (n = 4).

768

769 *Table S1: Summary of the parameters characterizing the oyster larvae analyzed in this study*

Variables	Description	Unit of measure	Abbreviation
Oyster variables			
Pediveligers	*Abundance of pre-settled pediveliger larvae on collector plates*	*ind. plate^{-1}*	*pediveligers*
Metamorphosed postlarvae	*Abundance of newly metamorphosed postlarvae on collector plates*	*ind. plate^{-1}*	*postlarvae*
Young settlers	*Abundance of pediveligers+ postlarvae on collector plates*	*ind. plate^{-1}*	*young settlers*
Juveniles	*Abundance of recruited juveniles on collector plates*	*ind. plate^{-1}*	*juveniles*
Prodissoconch II size	*Measurement of prodissoconch maximum shell height along maximal dorsoventral axis of larvae or juvenile Pacific oysters*	*µm*	*PII size*
Total fatty acids in young settlers	*Total fatty acid contents in larvae (young settlers)*	*ng lavae^{-1}*	*TFA*
Essential fatty acids	*Sum of essential fatty acids in larvae (docosahexaenoic acid (22:6ω3; DHA), eicosapentaenoic acid (20:5ω3; EPA) and arachidonic acid (AA))*	*ng lavae^{-1}*	*EFA*

770

771 *Table S2: Summary of the parameters characterizing the environment analyzed in this study.*

Variables	Description	Unity	Abbreviation
Environmental variables			
Temperature	*Discrete measure*	*°C*	*-*
Salinity	*Discrete measure*	*No unit*	*-*
Oxygen concentration	*Discrete measure*	*mg l^{-1}*	*-*
Total particulate matter$_{0.7\text{-}20\ \mu m}$	*Total particular pelagic material in the 0.7-20 µm fraction*	*mg l^{-1}*	*$TPM_{0.7\text{-}20\mu m}$*
Particulate organic matter$_{0.7\text{-}20\mu m}$	*Particulate pelagic material in fraction the 0.7-20 µm fraction*	*mg l^{-1}*	*$POM_{0.7\text{-}20\mu m}$*
Particulate inorganic matter$_{0.7\text{-}20\mu m}$	*Particulate inorganic pelagic material in the fraction 0.7-20 µm fraction*	*mg l^{-1}*	*$PIM_{0.7\text{-}20\mu m}$*
TFA content in $TPM_{0.7\text{-}20}$	*TFA content in $TPM_{0.7\text{-}20}$*	*µg mg $TPM_{0.7\text{-}20}^{-1}$*	
Total chlorophyll a	*Total chlorophyll a biomass*	*µgChla l^{-1}*	*~~chl~~Chloa*
Total chlorophyll b	*Total chlorophyll b biomass*	*µgChlb l^{-1}*	*~~chl~~Chlob*
Total chlorophyll c	*Total chlorophyll c biomass*	*µgChlc l^{-1}*	*~~chl~~Chloc*
Picophytoplankton biomass	*Chlorophyll a biomass in the <3 µm fraction (picoeukaryotes)*	*µgChla l^{-1}*	*pico_~~chl~~Chloa*
Nanophytoplankton biomass	*Chlorophyll a biomass in the 3-20 µm fraction (nanoeukaryotes)*	*µgChla l^{-1}*	*nano_~~chl~~Chloa*
Picophytoplankton+ nanophytoplankton	*Biomass*	*µgChla l^{-1}*	*nano_total_~~chl~~Chloa*
Microphytoplankton > 20 µm	*Biomass (microeukaryotes)*	*µgChla l^{-1}*	*micro_~~chl~~Chloa*
Bacteria	*Abundance of picocyanobacteria (<1 µm)*	*10^6 cell. l^{-1}*	*bacteria*
Total picoeukaryotes	*Abundance*	*10^6 cell. l^{-1}*	*peuk_tot*
picoeukaryotes+ cyanophyceae	*Abundance*	*10^6 cell. l^{-1}*	*pico_tot*
Nanophytoplankton	*Abundance*	*10^6 cell. l^{-1}*	*nano*
cryptophyceae	*Abundance*	*10^6 cell. l^{-1}*	*crypto*
Nanophytoplankton + cryptophyceae	*Abundance*	*10^6 cell. l^{-1}*	*nano_tot*
Heterotrophic flagellates	*Abundance*	*cell l^{-1}*	*HF*
Ciliates	*Abundance*	*cell l^{-1}*	*ciliates*
Tintinnidae	*Abundance*	*cell l^{-1}*	*tinti*
Diatoms	*Abundance*	*cell l^{-1}*	*diatom*
Dinoflagellates	*Abundance*	*cell l^{-1}*	*dinoflagellate*
Territorial competition by worms			
Worm coverage	*Percent cover of tubeworms (Ficopomatus enigmaticus) on plates*	*%*	*-*

772

773

Table S3: multivariate PERMANOVA investigating site and year effect for Temperature

Source	df	SS	MS	Pseudo-F	P(perm)	Unique perms	P(MC)
site	3	7,087	2,3623	1,158	0,3305	9951	0,3335
year	1	135,72	135,72	66,53	0,0001	9825	0,0001
position	1	3,2	3,2	1,5686	0,2085	9805	0,217
sitexyear	3	0,3865	0,12883	0,063154	0,9764	9951	0,9754
sitexposition	3	2,573	0,85767	0,42042	0,7357	9950	0,7371
yearxposition	1	1,1045	1,1045	0,54142	0,4681	9828	0,473
sitexyearxposition	3	0,0865	0,028833	0,014134	0,9977	9955	0,9977
Res	64	130,56	2,04				
Total	79	280,72					

Table S4: multivariate PERMANOVA investigating site, depth and year effect for salinity

Source	df	SS	MS	Pseudo-F	P(perm)	Unique perms	P(MC)
Site	3	5,331	1,777	7,5677	0,0002	9962	0,0004
Year	1	2,2445	2,2445	9,5587	0,0031	9805	0,0034
position	1	0,072	0,072	0,30663	0,5764	9733	0,5827
sitexyear	3	0,5245	0,17483	0,74457	0,5286	9960	0,5323
sitexposition	3	0,059	0,019667	0,083755	0,9666	9945	0,9679
yearxposition	1	0,1125	0,1125	0,47911	0,4824	9806	0,4966
sitexyearxposition	3	0,0805	0,026833	0,11428	0,9545	9942	0,9503
Res	64	15,028	0,23481				
Total	79	23,452					

Table S5: multivariate PERMANOVA investigating site, depth and year effect for oxygen

Source	df	SS	MS	Pseudo-F	P(perm)	Unique perms	P(MC)
site	3	3,8333	1,2778	1,3099	0,2739	9944	0,27
year	1	15,878	15,878	16,277	0,0004	9825	0,0001
position	1	10,039	10,039	10,292	0,002	9854	0,0018
sitexyear	3	10,01	3,3366	3,4205	0,0215	9947	0,0217
sitexposition	3	3,8499	1,2833	1,3156	0,2758	9955	0,2805
yearxposition	1	3,3048	3,3048	3,388	0,0708	9812	0,0682
sitexyearxposition	3	1,7959	0,59865	0,6137	0,6012	9955	0,5985
Res	64	62,43	0,97547				
Total	79	111,14					

Table S6: multivariate PERMANOVA investigating site and year effect for TPM

Source	df	SS	MS	Pseudo-F	P(perm)	Unique perms	P(MC)
site	3	1,493	0,49767	0,28089	0,8424	9962	0,8364
year	1	207,48	207,48	117,1	0,0001	9839	0,0001
sitexyear	3	2,0244	0,67479	0,38085	0,7691	9958	0,7708
Res	100	177,18	1,7718				
Total	107	388,6					

Table S7: multivariate PERMANOVA investigating site and year effect for PIM

Source	df	SS	MS	Pseudo-F	P(perm)	Unique perms	P(MC)
site	3	0,11747	0,039156	0,039431	0,9901	9949	0,9904
year	1	54,939	54,939	55,325	0,0001	9814	0,0001
sitexyear	3	0,33001	0,11	0,11077	0,957	9958	0,9508
Res	100	99,303	0,99303				
Total	107	154,73					

Table S8: multivariate PERMANOVA investigating site and year effect for POM

Source	df	SS	MS	Pseudo-F	P(perm)	Unique perms	P(MC)
site	3	1,4638	0,48793	2,796	0,0429	9952	0,0407
year	1	48,888	48,888	280,15	0,0001	9824	0,0001
sitexyear	3	1,193	0,39765	2,2787	0,0834	9952	0,0832
Res	100	17,451	0,17451				
Total	107	69,327					

Table S9: multivariate PERMANOVA investigating site, size and year effect for CHLOA

Source	df	SS	MS	Pseudo-F	P(perm)	Unique perms	P(MC)
site	3	3,35	1,1167	3,9887	0,0088	9958	0,0088
year	1	3,6519	3,6519	13,045	0,0003	9848	0,0007
taille	2	1,8257	0,91286	3,2608	0,0401	9953	0,0456
sitexyear	3	2,9083	0,96945	3,4629	0,0167	9953	0,0175
sitexsize	6	1,984	0,33066	1,1811	0,3199	9933	0,3246
yearxsize	2	5,0665	2,5333	9,0488	0,0004	9951	0,0004
sitexyearxsize	6	0,84964	0,14161	0,50582	0,8156	9949	0,8092
Res	96	26,876	0,27995				
Total	119	46,512					

Table S10: multivariate PERMANOVA investigating site and year effect for PEUK_TOT

Source	df	SS	MS	Pseudo-F	P(perm)	Unique perms	P(MC)
site	3	1,2885E+16	4,2951E+15	1,3441	0,2784	9945	0,2768
year	1	1,959E+16	1,959E+16	6,1306	0,0155	9835	0,0187
sitexyear	3	2,6684E+15	8,8948E+14	0,27835	0,8512	9952	0,8401
Res	32	1,0226E+17	3,1955E+15				
Total	39	1,374E+17					

Table S11: multivariate PERMANOVA investigating site, size and year effect for CYAN

Source	df	SS	MS	Pseudo-F	P(perm)	Unique perms	P(MC)
site	3	2,552E+16	8,5068E+15	0,7044	0,5664	9949	0,5635
year	1	5,3384E+17	5,3384E+17	44,205	0,0001	9851	0,0001
sitexyear	3	1,2146E+16	4,0486E+15	0,33524	0,8082	9953	0,797
Res	32	3,8645E+17	1,2077E+16				
Total	39	9,5796E+17					

Table S12: multivariate PERMANOVA investigating site, size and year effect for PICO

Source	df	SS	MS	Pseudo-F	P(perm)	Unique perms	P(MC)
site	3	2,3685E+15	7,8951E+14	0,083154	0,9729	9939	0,9697
year	1	7,5797E+17	7,5797E+17	79,832	0,0001	9841	0,0001
sitexyear	3	3,7254E+15	1,2418E+15	0,13079	0,9431	9944	0,938
Res	32	3,0383E+17	9,4946E+15				
Total	39	1,0679E+18					

Table S13 : multivariate PERMANOVA investigating site, size and year effect for NANO

Source	df	SS	MS	Pseudo-F	P(perm)	Unique perms	P(MC)
site	3	1,2396E+12	4,1319E+11	0,13497	0,9421	9944	0,9377
year	1	1,7765E+13	1,7765E+13	5,8032	0,0196	9837	0,0175
sitexyear	3	2,0028E+13	6,6759E+12	2,1807	0,1051	9950	0,1082
Res	32	9,7961E+13	3,0613E+12				
Total	39	1,3699E+14					

Table S14 : multivariate PERMANOVA investigating site, size and year effect for BACT_TOT

Source	df	SS	MS	Pseudo-F	P(perm)	Unique perms	P(MC)
site	3	1,622E+19	5,4066E+18	0,93657	0,4508	9949	0,4387
year	1	2,909E+20	2,909E+20	50,392	0,0001	9839	0,0001
sitexyear	3	1,0607E+19	3,5358E+18	0,61249	0,6213	9957	0,6151
Res	32	1,8473E+20	5,7728E+18				
Total	39	5,0246E+20					

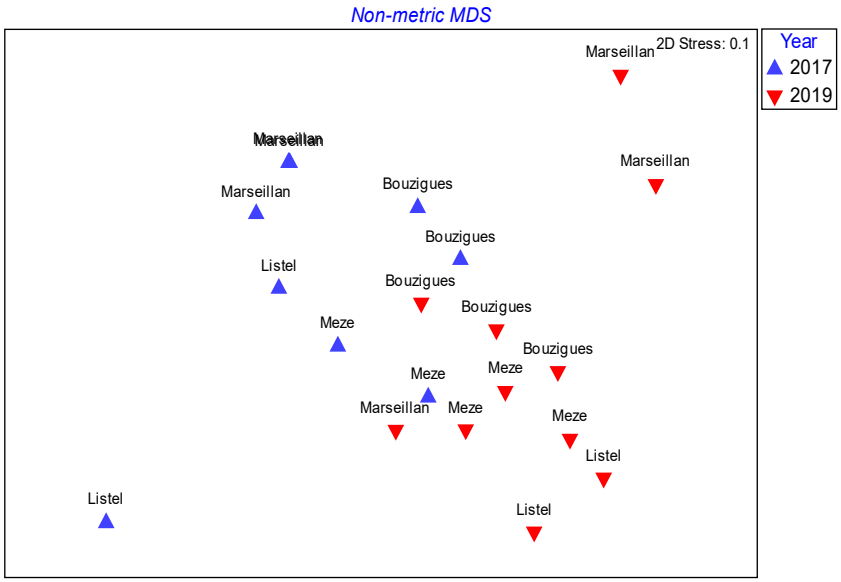

899

900 *Figure S1. Non-metric multidimensional scaling of the Euclidean similarity matrix based on the relative abundance of fatty*
901 *acid profiles measured in young settler larvae collected in 2017 and 2019 at each sampling site in the Thau lagoon.*

902